Department of the Navy
Office of Naval Research
Contract N6onr-244
Task Order II (NR 062-010)

POTENTIAL FLOW THROUGH RADIAL FLOW TURBOMACHINE ROTORS

A. J. Acosta

Hydrodynamics Laboratory
California Institute of Technology
Pasadena, California

Report No. E-19.4

February 1954

Table of Contents

Abstract

The exact theory of incompressible potential flow through pump impellers with logarithmic spiral (constant angle) blades is extended to include radial or conical turbomachines with small variations in vane angle and passage breadth. Approximate formulas are obtained and charts given for smooth entry and performance characteristics of pump or turbine configurations when the solidity is somewhat greater than unity and when the major blade deviations are confined to the inlet regions. However, the results of the present analysis are general and may be applied to blade rows with reasonably arbitrary camber lines.

I. Introduction

In recent years there has been some attention given to the problem of calculating the performance of compressor or pump impellers with a finite number of blades.[1, 2] By and large these efforts consist of solving field equations either by numerical methods (i.e. the relaxation technique) or by variations of stream filament theories. If compressibility effects must be considered it appears inevitable that such methods must be used, particularly if any of the flow details, e.g., velocity distributions, are desired. Furthermore, since the impeller geometries commonly employed are rather complex the question of analysis is made increasingly difficult. Although it is possible to obtain velocity and pressure fields for rather arbitrary configurations by the methods proposed in Refs. 1 and 2, the labor and time required for solutions are prohibitive for most engineering situations. Moreover, these calculations are for specific cases and do not permit generalizations to be made from them.

It was precisely because of these limitations that the earlier efforts of Spannhake[3] and Sörensen[4] were devoted to obtaining analytic solutions for impeller geometries of somewhat simplified shape. Spannhake obtained the incompressible, nonviscous head flow-rate characteristic for impellers with straight radial blades of arbitrary radius ratio with constant impeller breadth. Later, Sörensen extended the theory to include the effect of constant blade or

stagger angle, but was unable to obtain exact solutions in closed form for the overall performance parameters. A. Busemann[5] in 1928 finally solved this problem and obtained expressions for the head flow-rate equation as well as for the "shockless entry" condition. His analysis was restricted to the potential flow in "two-dimensional" impellers with a finite number of logarithmic spiral blades. These results are exact insofar as the results are given in series which may be calculated to any accuracy desired. Busemann's theory gives a good approximation for many cases provided the flow is predominantly radial or two-dimensional. However, most impellers are not two-dimensional nor are the impeller blades strictly logarithmic spirals.

It is to this last problem that this present work is mainly devoted. Unfortunately, a truly exact general analytic solution would involve great difficulties, so that approximations must be made. The program to be followed herein consists first of obtaining a more general form of Busemann's results by a slightly different method. Inasmuch as this theory is applicable to turbines as well as pumps both sets of coefficients will be given. It will then be seen that approximations in the spirit of the thin airfoil theory can be made. The approximate problem is then formulated and the results are given for small variations in blade shape and impeller breadth. It will also be shown that under certain conditions these results apply to flows over cones so that the present results may form the starting point for a theory of mixed flow impellers.

In the course of this work, approximate formulas may be obtained easily for the case of high solidity. These have been found to be extremely useful for a rapid estimate of the overall performance.

II. Formulation of the Problem

In this and the following three sections we work out the potential flow through a circular array of equally spaced logarithmic spiral blades. The breadth of the impeller is assumed to be constant. Under these conditions the flow is two-dimensional and hence the methods of conformal mapping may be used. An important simplification in this problem is that the flow due to the rotation of the blades may be treated separately from the through flow,

i.e., the flow responsible for net discharge through the runner. In this section the properties of the mapping function which enable these problems to be solved are worked out. In the succeeding sections the flow arising from the rotation of the blades in still water (displacement flow) and the through flow are obtained.

Mapping Function

The mapping function is[5]

$$z = \left[\frac{w_o - w}{w_o - 1}\right]^{\frac{1}{N}} \left[\frac{w_o - 1/w}{w_o - 1}\right]^{\frac{e^{2i\gamma}}{N}} \tag{1}$$

or,

$$\frac{dz}{z} = \frac{e^{i\gamma}}{N} \frac{dw}{w} \left[\frac{e^{i\gamma}/w}{\bar{w}_o - 1/w} - \frac{e^{-i\gamma} w}{\bar{w}_o - w}\right] . \tag{2}$$

It is easy to verify that Eq.(1) is the desired function since when w is on the unit circle Eq.(2) gives Arg $dz/z = \gamma$ which is precisely the equation of a logarithmic spiral. Moreover, Eq.(1) is a single valued function if $|w| \geq 1$ and the point w_o is not enclosed. If w_o is enclosed, once the argument of z increases by $2\pi/N$, thus moving a point in one blade passage to a congruent point in the next adjacent one, Fig. 1a. The point w_o is the complex constant and represents the origin of the physical plane. The point $w = \infty$ corresponds to $z = \infty$ also. This function is slightly different than the one usually used for annular or cascade flows.[6] The end points of the blade are given by the roots of $dz/dw = 0$. If the point corresponding to the exit tip of the blade is arbitrarily chosen as unity, then

$$\left.\begin{aligned} w_2 &= 1 \\ w_1 &= e^{i(2\gamma + 2\delta + \bar{u})} \end{aligned}\right\} \tag{3}$$

and

$$\left.\begin{aligned} w_o &= a e^{i\delta} \\ a &= \sin\gamma / \sin(\gamma + \delta) \end{aligned}\right\} \tag{4}$$

where w_1 corresponds to the inlet edge of the blade. From the above the exit radius of the blade $r_2 = |z_2| = 1$, thus the radius ratio of the impeller is given as $r_1/r_2 = |z_1|$ or using Eq.(1) one obtains

$$\frac{r_1}{r_2} = \left[- \frac{\sin(2\gamma+\delta)}{\sin\delta} \right]^{\frac{1+\cos 2\gamma}{N}} \cdot e^{-2\frac{(\pi-\delta-\gamma)}{N}\sin 2\gamma} \qquad (5)$$

For straight radial blades $\gamma = 0$ and Eq.(5) reduces to

$$\frac{r_1}{r_2} = \left[\frac{a-1}{a+1} \right]^{2/N} . \qquad (5a)$$

From Eq. 4

$$\tan\gamma = \frac{a \sin\delta}{1 - a\cos\delta}$$

from which Fig. 1b may be constructed. As an aid in determining the constants a and δ the following expressions are useful:

$$a^2 - 1 = \frac{2\cos^2\gamma}{\cosh\left[\frac{\sigma - 4\sin\gamma(\pi-\delta-\gamma)}{2\cos\gamma}\right] - 1} \qquad (5b)$$

where

$$\sigma = \frac{N \ln r_2/r_1}{\cos\gamma} .$$

In case $a \approx 1$, the relation

$$a^2 - 1 = 4\cos^2\gamma \; e^{-\frac{\sigma - 4\sin\gamma(\pi-\delta-\gamma)}{2\cos\gamma}} \qquad (5c)$$

may be used as an approximation. Equation (5b) is plotted in Fig. 2.

III. The Displacement Flow

In order that there be no flow through the surface of the blade, the velocity component of the flow normal to the blade must satisfy the condition

$$V_n = \underline{n} \cdot \underline{\omega} \times \underline{r}$$

where $\underline{n}$ is the outward normal of the blade surface. Thus the normal vector velocity must be

$$V_{nz} = \omega \cos\gamma \; z_b \, e^{i(\pi/2+\gamma)} \quad .$$

Let F be the complex potential of this flow. Then

$$\frac{dF}{dw} = \frac{dF}{dz} \cdot \frac{dz}{dw} \; ,$$

and dF/dz is the conjugate of the vector velocity V_z in the z-plane. Since polar coordinates must be used in the w-plane, we have as the boundary condition on the unit circle

$$V_{rw} \, e^{-i\theta} = \omega \cos\gamma \; \overline{z}_b \frac{dz_b}{dw} \; e^{-i(\pi/2+\gamma)} \quad . \tag{6a}$$

With the aid of Eq. (2) one obtains finally

$$V_{rw} = -i \, \frac{\omega \cos\gamma}{N} \; z_b \, \overline{z}_b \left[\frac{e^{i(\gamma-\theta)}}{\overline{w}_o - e^{-i\theta}} - \frac{e^{-i(\gamma-\theta)}}{w_o - e^{i\theta}} \right] \; , \tag{6b}$$

where

$$\left.\begin{aligned} z_b \, \overline{z}_b &= \left[\frac{w_o - e^{i\theta}}{w_o - 1} \right]^{\overline{q}} \left[\frac{\overline{w}_o - e^{-i\theta}}{\overline{w}_o - 1} \right]^{q} \\ q &= \frac{1}{N} \left(1 + e^{2i\gamma}\right) \quad . \end{aligned}\right\} \tag{6c}$$

The problem is now to find the corresponding tangential velocity

distribution on the unit circle subject to the additional restriction that this velocity vanish at infinity. The solution may be obtained in any number of ways. The most direct consists of writing the complex potential F in the form

$$F(w) = \sum_{n=0}^{\infty} A_n w^{-n} ,$$

and solving for the coefficients by means of Eq. 6b and hence obtaining the conjugate velocity $V_{\theta w}$. The procedure that will be followed herein is essentially the same as that outlined above and differs only in some details.

In order to effect a solution, the fact will be used that if the normal component of the velocity about the unit circle can be written as

$$\left.\begin{aligned} V_r &= f(e^{-i\theta}) + \overline{f}(e^{i\theta}) \\ \text{then the tangential velocity is} \\ V_\theta &= \frac{1}{i}\left[\overline{f}(e^{i\theta}) - f(e^{-i\theta})\right] \end{aligned}\right\} \qquad (7)$$

provided that the velocity should vanish at infinity. This statement is essentially a variation of Milne-Thompson's circle theorem.[7] Thus in order to obtain the conjugate velocity $V_{\theta w}$ all that must be done is to arrange Eq.(6b) in ascending and descending powers of $e^{i\theta}$ and then to apply Eq.(7). In Eq. (7), V_θ is frequently spoken of as the "conjugate function" or simply the conjugate of V_r.

Conjugation of the Displacement Flow

Since $|w_o| \geq 1$, the brackets in Eq. (6b) may be expanded by the binomial theorem. If the terms are arranged in positive and negative powers of $e^{i\theta}$ one obtains for the boundary condition in the w-plane

$$V_{rw} = -\frac{i\omega \cos\gamma}{N\,\Gamma(-q)\Gamma(-\overline{q})}\left[\frac{w_o}{w_o-1}\right]^{\overline{q}}\left[\frac{\overline{w}_o}{\overline{w}_o-1}\right]^{q}\left\{\sum_{n=0}^{\infty}\frac{\Gamma(n-q)\Gamma(n-\overline{q})}{n!\,n!\,|w_o|^{2n}}\right.$$

$$\left.+\sum_{k=1}^{\infty}\left[\frac{\overline{A}_k e^{ik\theta}}{w_o^{\,k}}+\frac{A_k e^{-ik\theta}}{\overline{w}_o^{\,k}}\right]\right\}\cdot\left\{\frac{e^{i(\gamma-\theta)}}{\overline{w}_o-e^{-i\theta}}-\frac{e^{-i(\gamma-\theta)}}{w_o-e^{i\theta}}\right\} \qquad (8)$$

where

$$A_k = \sum_{m=0}^{\infty} \frac{\Gamma(m+k-\bar{q})\Gamma(m-q)}{(m+k)!\ m!\ |w_o|^{2m}} \quad . \tag{9}$$

The following terms must now be conjugated:

$$S_1 = \sum_{n=0}^{\infty} \frac{\Gamma(n-q)\Gamma(n-\bar{q})}{n!\ n!\ |w_o|^{2n}} \left[\frac{e^{i(\gamma-\theta)}}{\bar{w}_o - e^{-i\theta}} - \frac{e^{-i(\gamma-\theta)}}{w_o - e^{i\theta}} \right] ,$$

$$S_2 = - \frac{\bar{A}_k}{i w_o^k} \cdot \frac{e^{-i\gamma} e^{i(k+1)\theta}}{w_o - e^{i\theta}} + \frac{A_k}{i \bar{w}_o^k} \cdot \frac{e^{i\gamma} e^{-i(k+1)\theta}}{\bar{w}_o - e^{-i\theta}}$$

and

$$S_3 = \frac{\bar{A}_k}{i w_o^k} \cdot \frac{e^{i\gamma} e^{i(k-1)\theta}}{\bar{w}_o - e^{-i\theta}} - \frac{A_k}{i \bar{w}_o^k} \cdot \frac{e^{-i\gamma} e^{-i(k-1)\theta}}{w_o - e^{i\theta}} \quad .$$

The terms S_1 and S_2 are easily conjugated by a straightforward application of Eq. (7). However, it is evident that if the denominator of S_3 is expanded by the binomial theorem then S_3 will contain terms of both positive and negative powers of $e^{i\theta}$. Thus in order to accomplish the conjugation it will be necessary to separate these terms. S_3 can be written as

$$S_3 = \frac{\bar{A}_k e^{i\gamma}}{i w_o^k} \sum_{n=1}^{\infty} \frac{e^{i(k-n)\theta}}{\bar{w}_o^n} + \text{conj. term}$$

with the aid of the geometrical series. Now if in the first sum

$$k - n = r = 0, 1, 2 \cdots \quad \text{for} \quad n \leq k$$

$$k - n = -r = 1, 2, 3 \cdots \quad \text{for} \quad n > k$$

then S_3 may be written in four separate terms as

$$S_3 = \frac{\bar{A}_k e^{i\gamma}}{i w_o^k} \sum_{r=0}^{k-1} \frac{e^{ir\theta}}{\bar{w}_o^{k-r}} - \frac{A_k e^{-i\gamma}}{i \bar{w}_o^k} \sum_{r=0}^{k-1} \frac{e^{-ir\theta}}{w_o^{k-r}}$$

$$+ \frac{\bar{A}_k e^{i\gamma}}{i w_o^k} \sum_{r=1}^{\infty} \frac{e^{-ir\theta}}{w_o^{k+r}} - \frac{A_k e^{-i\gamma}}{i \bar{w}_o^k} \sum_{r=0}^{\infty} \frac{e^{ir\theta}}{w_o^{k+r}} .$$

S_3 is now expressed in four sums which, taken two at a time, are arranged in ascending and descending powers of $e^{i\theta}$ as required by Eq. (7). It should be noted that the boundary condition on the blade must result in a flow which has no net source strength within the unit circle in the w-plane. Consequently, the terms corresponding to the index $r=0$ in S_3 are either zero or have a sum of zero. Hence, in treating S_3 this index is dropped.

The conjugation rule of Eq. (7) is now applied to terms S_1, S_2 and S_3 to obtain

$$S_1^* = \sum_{n=0}^{\infty} \frac{\Gamma(n-q)\,\Gamma(n-\bar{q})}{n!\, n!\, |w_o|^{2n}} \left[\frac{e^{i(\gamma-\theta)}}{\bar{w}_o - e^{-i\theta}} + \frac{e^{-i(\gamma-\theta)}}{w_o - e^{i\theta}} \right] ,$$

$$S_2^* = \frac{A_k e^{i(\gamma-\theta)}}{\bar{w}_o - e^{-i\theta}} \cdot \frac{e^{-ik\theta}}{\bar{w}_o^k} + \frac{\bar{A}_k e^{-i(\gamma-\theta)}}{w_o - e^{i\theta}} \cdot \frac{e^{ik\theta}}{w_o^k}$$

and

$$S_3^* = \frac{A_k e^{-i(\gamma-\theta)}}{w_o - e^{i\theta}} \left[\frac{2}{|w_o|^{2k}} - \frac{e^{-ik\theta}}{w_o^k} \right] + \frac{\bar{A}_k e^{i(\gamma-\theta)}}{\bar{w}_o - e^{-i\theta}} \left[\frac{2}{|w_o|^{2k}} - \frac{e^{ik\theta}}{w_o^k} \right]$$

$$+ \frac{1}{|w_o|^{2k}} \left[A_k e^{-i\gamma} + \bar{A}_k e^{i\gamma} \right]$$

where A_k is given by Eq. (9). The resultant sum of these terms may be considerably simplified by the use of the addition theorem for binomial coefficients

which in the form suitable for use here is

$$\frac{1}{\Gamma(-a)} \sum_{m=o}^{S} \frac{\Gamma(m-a)}{m!} = -\frac{(S-a)}{a\Gamma(-a)} \cdot \frac{\Gamma(S-a)}{S!} \quad .$$

The result of these operations is

$$V_{\theta w} = \frac{\omega \cos\gamma}{N} \left[\frac{w_o}{w_o - 1}\right]^{\bar{q}} \left[\frac{\bar{w}_o}{\bar{w}_o - 1}\right]^{q} \left\{ \left[\frac{e^{i(\gamma-\theta)}}{\bar{w}_o - e^{-i\theta}} - \frac{e^{-i(\gamma-\theta)}}{w_o - e^{i\theta}} \right] F_1 - \frac{N}{\cos\gamma} \right.$$

$$\left. \cdot \left[1 + \frac{e^{i\theta}}{w_o - e^{i\theta}} + \frac{e^{-i\theta}}{\bar{w}_o - e^{-i\theta}} \right] F_2 + \left[\frac{e^{i(\gamma-\theta)}}{\bar{w}_o - e^{-i\theta}} - \frac{e^{-i(\gamma-\theta)}}{w_o - e^{i\theta}} \right] \right.$$

$$\left. \cdot \sum_{m=o}^{\infty} \sum_{n=1}^{\infty} \left[\frac{\Gamma(m+n-q)\Gamma(m-\bar{q})\, e^{-in\theta}}{(m-n)!\; m!\; |w_o|^{2m}\; \bar{w}_o^{-n}} - \frac{\Gamma(m+n-\bar{q})\Gamma(m-q)\, e^{in\theta}}{(m+n)!\; m!\; |w_o|^{2m}\; w_o^{n}} \right] \right\} \qquad (10a)$$

where F_1, F_2 are hypergeometric functions defined by

$$F_1 = F\left(-q, -\bar{q}; 1; \frac{1}{|w_o|^2}\right), \quad F_2 = \lim_{\epsilon \to 0} \left[F\left(-q, -\bar{q}; \epsilon; \frac{1}{|w_o|^2}\right) \right] .$$

and F is given by the series[9]

$$F(a, b; c; z) = \frac{\Gamma(c)}{\Gamma(a)\Gamma(b)} \sum_{n=o}^{\infty} \frac{\Gamma(a+n)\Gamma(b+n)}{n!\,\Gamma(c+n)}\, z^n \quad . \qquad (10b)$$

Unfortunately, there seems to be no way to reduce the double series to a single series. However, this equation does provide the displacement flow velocity distribution around the impeller blades and in any specific case presumably these terms could be evaluated. Equation (10a) represents only part of the complete displacement flow, for in order to establish lift or torque, the Kutta condition must be prescribed at the exit tip for a pump or at the inlet edge (w_1) for a turbine. Consequently, in determining the head-flow rate characteristics the values of $V_{\theta_1 w}$ and $V_{\theta_2 w}$ will be needed, i.e., those

velocities corresponding to the exit and inlet blade tips. Fortunately, the factor of the double series (Eqs. (10)) vanishes at these points. Let V_{d_2} and V_{d_1} denote the tangential displacement velocities at the exit and inlet tips. They become

$$V_{d_2} = - \frac{\omega \cos\gamma}{N \rho_2} \left[\frac{w_o}{w_o - 1}\right]^{\bar{q}} \left[\frac{\bar{w}_o}{\bar{w}_o - 1}\right]^{q} \left[2F_1 + \frac{N}{\cos\gamma}(\rho_2 - 2\cos\gamma) F_2\right], \tag{11a}$$

and

$$V_{d_1} = \frac{\omega \cos\gamma}{N \rho_1} \left[\frac{w_o}{w_o - 1}\right]^{\bar{q}} \left[\frac{\bar{w}_o}{\bar{w}_o - 1}\right]^{q} \left[2F_1 - \frac{N}{\cos\gamma}(\rho_1 + 2\cos\gamma) F_2\right] \tag{11b}$$

where

$$\rho_2 = |w_o - 1|, \quad \rho_1 = |w_o - w_1| \quad . \tag{12}$$

Equations (11) are Busemann's principle results.

IV. The Through Flow

In this section the flow from a source-vortex through the stationary (nonrotating) array of blades is worked out. Inasmuch as the through flow for normal pumping and turbining is slightly different they will be discussed separately.

a. Pump. The point w_o represents the origin in the z-plane, and all of the through flow is supposed to originate there. In the w-plane the solution of this flow is obtained by imaging a source vortex at w_o in the unit circle. This flow potential is

$$G(w) = \frac{A}{2\pi} \log(w - w_o) + \frac{\bar{A}}{2\pi} \log\left(\frac{1}{w} - \bar{w}_o\right) \tag{13}$$

where $A = Q + i\Gamma$, Q and Γ being the source and vortex strength respectively. In order to see the significance of A let $w \to w_o$ so that $z \to 0$. Then from Eq. (1)

$$w_o - w \longrightarrow \text{const} \times z^N$$

Hence, near the origin in the z-plane

$$G(z) \longrightarrow \frac{A}{2\pi} \log z^N = \frac{N}{2\pi}(Q + i\Gamma)(\log |z| + i \operatorname{Arg} z) ,$$

and the stream function is

$$\Psi = \frac{N}{2\pi}(\Gamma \log |z| + Q \operatorname{Arg} z) .$$

The angle between a radial line and the tangent to the streamline is given by

$$\tan \alpha_1 = r \frac{d\nu}{dr} = -\Gamma/Q , \tag{14}$$

where α is positive as shown in Fig. 3. Hence, it can be seen that the streamlines issue from the origin on logarithmic spirals inclined at an angle α_1 to any radius.

The velocities on the unit circle may be found by differentiation of Eq. (13) and they are found to be

$$V_{r_w} - i V_{\theta_w} = \frac{Q}{2\pi} \left[(1 - i \tan \alpha_1) \frac{w}{w - w_o} - \frac{1 + i \tan \alpha_1}{w^2 (\frac{1}{w} - w_o)} \right] .$$

The radial velocity is zero as it should be and upon reference to Fig. 1b it can be seen that for $w = 1$

$$V_{t_2} = -\frac{Q \cos \gamma}{\pi \rho_2} (\tan \gamma - \tan \alpha_1) \tag{15a}$$

and similarly,

$$V_{t_1} = \frac{Q \cos \gamma}{\pi \rho_1} (\tan \gamma - \tan \alpha_1) . \tag{15b}$$

b. Turbine. In the case of a pump the flow issues from the origin and approaches the blades with a prewhirl characterized by the angle α_1. However, in normal turbine operation the flow progresses radially inwards and approaches the impeller with a given angle α_2 positive in the same sense as α_1. The potential for this flow is obtained by merely replacing Q by $-Q$ in Eq. (13). Thus,

$$\tan \alpha_2 = \Gamma/Q \tag{16}$$

for a turbine and also

$$V_{t_2} = \frac{Q \cos \gamma}{\pi \rho_2} \quad (\tan \gamma - \tan \alpha_2) \tag{17a}$$

$$V_{t_1} = - \frac{Q \cos \gamma}{\pi \rho_1} \quad (\tan \gamma - \tan \alpha_2) \quad , \tag{17b}$$

for the velocities at the exit and inlet blade tips.

In the development of the characteristic head equation for a turbine we shall need to use an expression for the circulation which must be put around the blades in order to satisfy the Kutta condition at the inner blade edge ($w = w_1$). However, this flow differs from that of a pump inasmuch as it must not disturb the flow conditions at infinity. Consequently, the potential for this flow in the w-plane must consist of a vortex at the point w_o with an image at the inverse point within the circle. Thus if H is this potential,

$$H(w) = i \frac{\Gamma_T}{2\pi} \log (w - w_o) - \frac{i \Gamma_T}{2\pi} \log (w - 1/\overline{w}_o) . \tag{18}$$

The velocities at the outer and inner blade tips are then respectively

$$V_{\Gamma_2} = \frac{\Gamma_T}{2\pi} \quad \frac{\rho_2 - 2 \cos \gamma}{\rho_2} \tag{19a}$$

$$V_{\Gamma_1} = \frac{\Gamma_T}{2\pi} \quad \frac{\rho_1 + 2 \cos \gamma}{\rho_1} \tag{19b}$$

where Γ_T is the strength of this vortex.

V. The Head Flow-Rate Equation

a. Pump. From elementary considerations the head of a pump can be shown to be

$$H = \frac{U_2 \overline{V}_{u2} - U_1 \overline{V}_{u1}}{g}$$

where $\overline{V_{u_2}}$, $\overline{V_{u_1}}$ are average values of the peripheral component of the absolute velocities in the direction of rotation at the exit and inlet. The head is usually expressed in terms of the dimensionless coefficient

$$\psi = H/U_2^2/g ,$$

and can be shown to be equal to

$$\psi = - \frac{\Gamma_2 - \Gamma_1}{2\pi r_2^2 \omega}$$

where Γ_2, Γ_1 are the values of the circulation at the outside and inside of the impeller. If Γ_z is the strength of the circulation about each of the N blades then this coefficient is

$$\psi = - \frac{N \Gamma_z}{2\pi r_2^2 \omega} .$$

As yet there is presumed to be no circulation around each of the blades. In order to fix the value of Γ_z the Kutta condition will be imposed at the exit tip of the blade, i.e., it will be assumed that the value of the velocity must be finite there. In the circle plane this condition is that the velocity at $w = 1$ must be zero. This condition may be satisfied without altering the boundary conditions by placing a vortex at the origin in the w-plane of such strength that

$$V_{d_2} + V_{t_2} - \frac{\Gamma_z}{2\pi} = 0 .$$

Thus,

$$\psi = - \frac{N}{\omega} (V_{d_2} + V_{t_2})$$

since r_2 is taken as unity. The first term is independent of flow rate and is incorporated into the constant ψ_o. The second term depends only on flow rate where Q is the discharge per passage. In terms of the dimensionless flow rate coefficient

$$\varphi = \frac{V_{r_2}}{U_2} = \frac{N Q}{2\pi r_2 \omega}$$

the head equation assumes the form

$$\psi = \psi_o + \varphi C_H (\tan \gamma - \tan \alpha_1) \tag{20a}$$

for forward curved blades ($\gamma > 0$) and

$$\psi = \psi_o - \varphi C_H (\tan \gamma - \tan \alpha_1) \tag{20b}$$

for backward curved blades ($\gamma < 0$). The shut-off head coefficient ψ_o is found from Eq. (11a) to be

$$\psi_o = C_H \left[\frac{a C_H}{2 \cos \gamma}\right]^{\frac{4 \cos^2 \gamma}{N}} \exp \left[- \frac{2 \sin 2\gamma}{N} (\pi - \gamma - \delta) \right] \cdot \left[F_1 + N \left(\frac{1}{C_H} - 1 \right) F_2 \right] \tag{21}$$

where

$$C_H = \frac{2 \cos \gamma}{P_2} = \frac{2a \sin \delta \cot \gamma}{1 + a^2 - 2a \cos \delta} . \tag{22}$$

This coefficient represents the effectiveness of the blades in guiding the flow whereas ψ_o represents the effectiveness in bringing up the average circumferential velocity to the impeller tip speed. It is evident from Eq. (21) and Fig. 1b that $0 \leq C_H \leq 1$. Values of the coefficient C_H are plotted in Ref. 8 and a more detailed plot is given herein in Fig. 5.

For particular values of r_1/r_2, γ and N, a, q, and σ may be determined either from Eq. (5b) or Fig. 2. The value of the functions F_1 and F_2 may then be found through the use of the series expansion Eq. (10b) in order to obtain ψ_o. Values of this coefficient are also plotted in Ref. 8 for various values of r_1/r_2, N and γ. However, these graphs, although quite useful, are not too accurate and since in the region of major interest relatively simple expressions may be developed for the shut-off head coefficient, the following paragraphs will be devoted to obtaining more convenient formulas and charts.

Calculation of values of ψ_o

It is clear from Fig. 2 that if the number of blades is small and the

radius ratio r_1/r_2 near unity, then the parameter a^2 is large and consequently the expansion of the hypergeometric functions F_1, F_2 will contain only a few terms so that these cases may be easily worked out. However, the majority of cases for pump and turbine applications turn out to be in the range of the parameter $1 \leq \sigma/2\pi \leq 2$. An inspection of Fig. 2 shows that the quantity $|w_o|^2 = a^2$ is about unity for these conditions. This situation is fortunate because the hypergeometric functions F_1, F_2 permit easy expansions to be made when the argument is near unity. In particular, the expansion around the point 1 of the hypergeometric function is[9]

$$F(a,b,c,x) = \frac{\Gamma(c)\,\Gamma(c-a-b)}{\Gamma(c-a)\,\Gamma(c-b)}\,F(a,b;1+a+b-c;1-x) + \frac{\Gamma(c)\,\Gamma(a+b-c)}{\Gamma(a)\,\Gamma(b)}(1-x)^{c-a-b}$$

$$\cdot\, F(c-a,\, c-b;\, 1+c-a-b;\, 1-x) \qquad (23)$$

provided none of a, b, c are negative integers.

Let $\frac{1}{a^2} = 1 - \Delta$, then the two sums F_1, F_2 become

$$F_1 = \frac{\Gamma(1+q+\bar{q})}{\Gamma(1+q)\,\Gamma(1+\bar{q})}\left[1 - \frac{q\bar{q}}{q+\bar{q}}\,\Delta - \frac{q\bar{q}(1-q)(1-\bar{q})}{2(1-q-\bar{q})(q+\bar{q})}\,\Delta^2 - \cdots\right]$$

$$- \frac{\sin\pi q \sin\pi\bar{q}}{\pi \sin\pi(q+\bar{q})}\;\frac{\Gamma(1+q)\,\Gamma(1+\bar{q})}{\Gamma(2+q+\bar{q})}\,\Delta^{1+q+\bar{q}}\left[1 + \frac{(1+q)(1+\bar{q})}{2+q+\bar{q}}\,\Delta + \cdots\right] \qquad (24a)$$

$$F_2 = \frac{\Gamma(1+q+\bar{q})}{N\,\Gamma(1+q)\,\Gamma(1+\bar{q})}\left[1 + \frac{q\bar{q}}{1-q-\bar{q}}\,\Delta + \cdots\right] - \frac{\sin\pi q \sin\pi\bar{q}}{\pi \sin\pi(q+\bar{q})}\;\frac{\Gamma(1+q)\,\Gamma(1+\bar{q})}{\Gamma(1+q+\bar{q})}\,\Delta^{q+\bar{q}}$$

$$\cdot\left[1 + \frac{q\bar{q}}{1+q+\bar{q}}\,\Delta + \cdots\right] \qquad (24b)$$

With the aid of Fig. 2, F_1 and F_2 may be simply computed for any given case. Again as is evident from Fig. 2, $\Delta \approx a^2 - 1$ becomes quite small and nearly independent of γ for about $\sigma/2\pi > 1.2$. Since Eqs. (24) depend largely on $1/a^2$, it can be seen that both they and the coefficient ψ_o will

rapidly approach the limiting value given by $a = 1$. If then, only first order terms in Δ are retained

$$\Psi_{o_{max}} = C_H \frac{\exp\left(-\frac{2\gamma \sin 2\gamma}{N}\right)}{(2\cos\gamma)^{\frac{4\cos^2\gamma}{N}}} \left\{ \frac{\Gamma(1+q+\bar{q})}{\Gamma(1+q)\,\Gamma(1+\bar{q})} \left[1 - \frac{\Delta}{N} \right] + \right.$$

$$\left. + \frac{\Delta}{4\cos^2\gamma} \left[\frac{\Gamma(1+q+\bar{q})}{\Gamma(1+q)\,\Gamma(1+\bar{q})} - \frac{\Gamma(1+q)\,\Gamma(1+\bar{q})}{\Gamma(1+q+\bar{q})} (\Delta)^{\frac{4\cos^2\gamma}{N}} \right] \right\} , \tag{25a}$$

and

$$C_H = 1 - \frac{\Delta}{4\cos^2\gamma} , \tag{26}$$

or more approximately

$$\Psi_{o_{max}} = \frac{\exp\left(-\frac{2\gamma \sin 2\gamma}{N}\right)}{(2\cos\gamma)^{\frac{4\cos^2\gamma}{N}}} \frac{\Gamma(1+q+\bar{q})}{\Gamma(1+q)\,\Gamma(1+\bar{q})} \tag{25b}$$

The gamma function factor may be directly calculated from its product definition, however a convenient expansion for it is

$$\frac{\Gamma(1+q+\bar{q})}{\Gamma(1+q)\,\Gamma(1+\bar{q})} = \exp\left[6.5797 \frac{\cos^2\gamma}{N^2} - 19.233 \frac{\cos^4\gamma}{N^3} \right.$$

$$\left. + 8.6584 \frac{\cos^4\gamma}{N^4} (8\cos^2\gamma - 1) + \cdots \right] . \tag{27}$$

Although this series diverges for $\frac{4\cos^2\gamma}{N} > 1$ it is rapidly convergent for values of this parameter less than about a quarter. For $\gamma = \pi/2$, q is real and any of the tables of the gamma function may be used.[10] From Eq. (25b)

it can be seen that $\psi_o \leq 1$, and the equality sign only holds for the case of $N = \infty$.

Figure 6 is a plot of the limiting or maximum value of ψ_o figured from Eq. (25b) vs. the blade angle γ for various numbers of blades. If the geometrical parameter $\sigma/2\pi$ is less than about unity, more accurate values of the shut-off head coefficient can be computed from Eq. (25a). However the proportions of most designs are such that Fig. 6 gives a good estimate of this parameter.

Condition of shockless entry

The head flow-rate characteristic (Eqs. (20)) is a straight line and in potential flow any point on that line could be achieved in operation. However, in the flow of a real fluid, large viscous effects may be expected to occur for highly unfavorable pressure gradients in the inlet portions of the impeller. For forward curved blades, an infinite velocity always occurs at the blade inlet edge, however for backward curved blades there is one flow rate for which finite velocities result at the inlet and this condition is variously known as "smooth entry" or "shockless entry". For shockless entry, then, the velocity is finite everywhere on the blade and presumably real fluid effects should be minimized at or near this operating point, other things being equal. Hence, the present calculations should be expected to give the best design predictions at or near smooth entry.[11]

In the w-plane $V(\theta_1) = 0$ for shockless entry and hence

$$V_{d_1} + V_{t_1} - \frac{\Gamma_z}{2\pi} = 0$$

is the condition that must be satisfied. The value of the circulation Γ_z can be expressed in terms of the exit velocities so that

$$(V_{d_1} - V_{d_2}) + (V_{t_1} - V_{t_2}) = 0$$

is the requirement. From Eqs. (15)

$$V_{t_1} - V_{t_2} = \frac{Q \cos\gamma}{\pi} (\tan\gamma - \tan\alpha_1)\left(\frac{1}{\rho_1} + \frac{1}{\rho_2}\right)$$

and from Eqs. (11)

$$V_{d_1} - V_{d_2} = \frac{2\omega\cos\gamma}{N}\left[\frac{w_o}{w_o - 1}\right]^{\bar{q}}\left[\frac{\bar{w}_o}{\bar{w}_o - 1}\right]^{q}(F_1 - NF_2)\left(\frac{1}{\rho_1} + \frac{1}{\rho_2}\right) .$$

Hence,

$$\frac{NQ}{2\pi\omega}(\tan\gamma - \tan\alpha_1) = -\left[\frac{w_o}{w_o - 1}\right]^{\bar{q}}\left[\frac{\bar{w}_o}{\bar{w}_o - 1}\right]^{q}(F_1 - NF_2) . \qquad (28a)$$

As before, most interest is usually in the case of $\sigma/2\pi > 1$ or $a^2 - 1 << 1$. In this event Eq. (28) may be evaluated with the use of Eqs. (5c) and (24). Then,

$$F_1 - NF_2 = \frac{N\sin\pi q \sin\pi\bar{q}}{\pi\sin\pi(q+\bar{q})}\;\frac{\Gamma(1+q)\,\Gamma(1+\bar{q})}{\Gamma(1+q+\bar{q})}(a^2-1)^{\frac{4\cos^2\gamma}{N}} - \frac{\Gamma(1+q+\bar{q})}{\Gamma(1+q)\,\Gamma(1+\bar{q})}\cdot\frac{a^2-1}{N}$$

or for $4\cos^2\gamma/N << 1$

$$F_1 - NF_2 = \left(1 + \frac{8\pi^2\cos^2\gamma}{6N^2}\right)\frac{\Gamma(1+q)\,\Gamma(1+\bar{q})}{\Gamma(1+q+\bar{q})}(4\cos^2\gamma)^{\frac{4\cos^2\gamma}{N}}\exp\left(\frac{4\gamma\sin 2\gamma}{N}\right)\left(\frac{r_1}{r_2}\right)^2 .$$

Equation 28 can now be put into the more usable form

$$\varphi_e(\tan\gamma - \tan\alpha_1) = -\frac{1}{\psi_{o_{max}}}\left(1 + \frac{8\pi^2\cos^2\gamma}{6N^2}\right)\left(\frac{r_1}{r_2}\right)^2 \qquad (28b)$$

with an error of less than 2 percent if $\sigma/2\pi > 1.2$ or so, since the next term gives an additional factor of

$$1 + \frac{8\cos^2\gamma}{N}\exp\left(-\frac{\sigma - 4\gamma\sin\gamma}{2\cos\gamma}\right)$$

which amounts to about a percent at most for the case considered here.

The significance of Eq. (28a) is brought out by noting that for the simple infinite vane theory

$$\varphi_{e_\infty}(\tan\gamma - \tan\alpha_1) = -\left(\frac{r_1}{r_2}\right)^2$$

in which the subscript ∞ denotes an infinite number of blades. Thus we have

$$\frac{\varphi_e}{\varphi_{e_\infty}} = \frac{1}{\psi_{o_{max}}} \left(1 + \frac{4\pi^2 \cos^2 \gamma}{3 N^2}\right) . \tag{29}$$

Since $\psi_o \leq 1$ it is evident that the flow rate for smooth entry always occurs at a flow rate greater than predicted by the infinite vane theory. This correction is important since from Fig. 6 typical values of $\psi_{o_{max}}$ may be 0.65 to 0.8. Thus if corrections are not allowed for, errors of 30 percent may be made.

Figure 7 is a plot of the head characteristic equation (Eq. (20)) for forward curved and backward curved vanes.

b. Turbine. The same considerations are used in developing the characteristics for turbines as for a pump. In fact if the flow-rate is sufficiently high for a pump with backward curved blades, a brief inspection of Fig. 7 will show that the head is negative and hence power is being taken out of the flow. However, turbines normally operate with the flow directed radially inwards, and the above situation is termed "reverse turbine" operation. In the condition of normal operation, then, the flow is inward and hence the Kutta condition must be applied at the inner blade edges.

The head drop across the impeller will be the same as for a pump, namely

$$\psi = - \frac{N \Gamma_z}{2\pi r_2^2 \omega}$$

The Kutta condition at the inner blade edge (w_1) requires that

$$V_{t_1} + V_{d_1} + V_{\Gamma_1} = 0 .$$

With the aid of Eqs. (11b), (17b) and (19b) one obtains in a manner similar to that of Eq. (20a)

$$\psi_T = \varphi C_H (\tan \gamma - \tan \alpha_2) - \psi_{o_T} \tag{30}$$

where

$$\psi_{oT} = \frac{\cos\gamma}{\rho_2}\left[\frac{w_o}{w_o - 1}\right]^{\bar{q}}\left[\frac{\bar{w}_o}{\bar{w}_o - 1}\right]^{q}\left[2F_1 - \frac{N}{\cos\gamma}(\rho_1 + 2\cos\gamma)F_2\right] . \quad (31)$$

The subscript "oT" refers to the turbine "shut-off head".

It is of interest to note that for values of φ where

$$\varphi \leq \psi_{oT}/C_H(\tan\gamma - \tan\alpha_2)$$

the head of the fluid increases in passing through the turbine and thus we have the analog to the reverse turbine, namely, the inward flow pump.

As in the case of the pump, most turbine configurations have values of the parameter $\sigma/2\pi > 1.2$ which means that $a \approx 1$ and $\rho_1 \approx 0$. In this event ψ_{oT} can be closely approximated by

$$\psi_{oT} = C_H\left[\frac{w_o}{w_o - 1}\right]^{\bar{q}}\left[\frac{\bar{w}_o}{\bar{w}_o - 1}\right]^{q}(F_1 - NF_2) .$$

This expression is seen to be nearly the same as that of Eq. (28a) so that one has approximately

$$\psi_{oT} = \frac{C_H}{\psi_{o_{max}}}\left(1 + \frac{4\pi^2\cos^2\gamma}{3N^2}\right)\left(\frac{r_1}{r_2}\right)^2 . \quad (32)$$

The behavior of the turbine shut-off coefficient is thus similar to that of the flow-rate for shockless entry of a pump.

Figure 8 is a plot of the characteristic equation (Eq. (30)) for a turbine for various values of α_2. For normal operation $\alpha_2 < 0$ and the sense of rotation is opposite to that of a pump with backward curved blades. The condition of no leaving whirl usually represents a useful approximation of the design operating point for most configurations. This condition is easily obtained from the inlet velocity triangle to be

$$\frac{\psi}{\varphi} = -\tan\alpha_2 .$$

Shockless entry

Reaction turbines, in general, have blade shapes which differ substantially from that of a logarithmic spiral so that smooth entry calculations based on the present theory are not too meaningful except possibly for a pump of conventional design run as a normal turbine. In this case, the calculation proceeds in the same manner as that leading to Eq. (28a), i.e., the condition $V(\theta = 0) = 0$ must be satisfied. When this occurs, the velocity at both the outer and inner blade edges is finite and it is clear that this condition corresponds exactly to that of a pump operating at shockless entry except that the direction of flow and rotation are reversed. Since the Kutta condition is satisfied at both points, the flow is reversible and the shockless entry computations for a pump can be applied to turbine operation.

Torque characteristics

Turbine performance is not usually presented in terms of the dimensionless head and flow coefficients ψ and φ unless the speed is maintained constant. If the speed is not constant, torque is given as a function of angular speed with either the head or flow-rate kept constant. In the present work it is most convenient to hold the discharge constant. The torque can then be expressed by means of the dimensionless coefficient χ

$$\chi = \frac{T}{\rho A_2 Q r_2 V_{r_2}} = \psi/\varphi \qquad (33)$$

where here ρ signifies density. In the case of a real fluid the efficiency is given by

$$\eta_T = \frac{\chi\varphi}{\psi} \quad .$$

This torque coefficient is to be distinguished from that of a pump operated at constant speed which is given by

$$\tau = \psi\varphi$$

and where the efficiency is given

$$\eta_p = \frac{\varphi\psi}{\tau} \quad .$$

The torque coefficient can be expressed as

$$\chi = C_H (\tan\gamma - \tan\alpha_2) - \frac{\psi_{oT}}{\varphi} \qquad (34)$$

with the use of Eq. (30). Thus χ is a straight line function of $1/\varphi$. The intercept of $\frac{1}{\varphi} = 0$ represents the locked rotor torque, and the value of $1/\varphi$ for $\chi = 0$ represents the turbine runaway speed. These results are shown in Fig. 9.

VI. Extension to Nonlogarithmic Spiral Shapes

The theory as presented thus far is limited to flow in strictly two-dimensional radial turbomachines. The simplified shapes demanded by this theory are seldom realized in actual designs. There is no doubt that the effects of blade angle and passage breadth variations, in addition to meridional curvature can cause important deviations from the two-dimensional theory. The flow through an arbitrary cascade of airfoils is a related but simpler problem and it has received great attention in the past twenty years. Unfortunately, it is quite difficult to get an exact analytic solution even for a circular arc profile although special cases may be worked out by Garrick's procedure.[12] This difficulty was partially circumvented by employing approximate methods similar to that of the thin airfoil theory. The work of Rannie[13] is among the most useful of these except that it is restricted to circular arc camber lines. Integrals for other shapes have been given by Pistolesi[14] but not evaluated.

There seems to have been relatively little analytical work done for an arbitrary radial array of pump blades. Calculation schemes using Ackeret's method of the continuous distribution of singularities have been worked out for pumping configurations by Betz and Flügge-Lotz,[15] but this method does not permit general analytic solutions to be obtained.

In the sections that follow a theory for nonlogarithmic spiral blades will be outlined. Like the work of Rannie and Pistolesi it is based on the ideas of thin airfoil theory. As the starting point for this method the solution of a more general boundary condition than Eq. (6) will be obtained. These new

solutions are then interpreted from the point of view of perturbations on a logarithmic spiral and correction terms for the head and flow-rate equation are obtained. The resulting blade shapes can be quite general and no restriction to any particular variation is necessary. These solutions are also embodied in further approximations to account for the non-uniform breadth of most impellers. Finally, a simple correction for nonradial, i.e., conical flows is given.

a. Solution for any Power Boundary Condition

Suppose that on the surface of the blade (Section II) the normal velocity is to be

$$|V_n| = k\omega\cos\gamma \; r^{m+1} \tag{35}$$

where r, ω, γ have the same meaning as before and k, m are real constants. The vector velocity is then

$$V_{nz} = k\omega\cos\gamma \; z_b \; |z_b|^m \; e^{i(\pi/2+\gamma)} ,$$

and following the procedure leading to Eq. (6b) the radial velocity in the w-plane becomes

$$V_{rw} = -i\frac{k\omega\cos\gamma}{N} z_b \bar{z}_b \; |z_b|^m \left[\frac{e^{i(\gamma-\theta)}}{\bar{w}_o - e^{-i\theta}} - \frac{e^{-i(\gamma-\theta)}}{w_o - e^{i\theta}}\right] .$$

Now

$$z_b \bar{z}_b \; |z_b|^m = |z_b|^{m+2} ,$$

and since $|z_b|^2$ is given by Eq. (6c), $|z_b|^{m+2}$ may be found by replacing 2 by m+2 to get

$$|z_b|^{m+2} = \left[\frac{w_o - e^{i\theta}}{w_o - 1}\right]^{\frac{m+2}{2}\bar{q}} \left[\frac{\bar{w}_o - e^{-i\theta}}{\bar{w}_o - 1}\right]^{\frac{m+2}{2}q} .$$

Thus the radial velocity in the circle plane can be written as

$$V_{rw} = -i\frac{k\omega\cos\gamma}{N} \left[\frac{w_o - e^{i\theta}}{w_o - 1}\right]^{\bar{q}'} \left[\frac{\bar{w}_o - e^{-i\theta}}{\bar{w}_o - 1}\right]^{q'} \left[\frac{e^{i(\gamma-\theta)}}{\bar{w}_o - e^{-i\theta}} - \frac{e^{-i(\gamma-\theta)}}{w_o - e^{i\theta}}\right] , \tag{36}$$

where

$$q' = \frac{1}{N'}\left(1 + e^{2i\gamma}\right) , \tag{37a}$$

or

$$N' = \frac{2}{m+2} N . \tag{37b}$$

The geometrical constants of the mapping are still determined by N, r_1/r_2 and γ. Equation (36) is now formally the same as (6b) except that q has been replaced by q'. The tangential velocity corresponding to boundary condition Eq. (36) is the same as Eq. (11) except that q and quantities derived from it are replaced by q'. Thus

$$V_2' = - \frac{k\omega\cos\gamma}{N\rho_2} \left[\frac{w_o}{w_o - 1}\right]^{\bar{q}'} \left[\frac{\bar{w}_o}{\bar{w}_o - 1}\right]^{q'} \left[2F_1 + \frac{N'}{\cos\gamma}(\rho_2 - 2\cos\gamma)F_2\right] , \tag{38a}$$

and

$$V_1' = \frac{k\omega\cos\gamma}{N\rho_1} \left[\frac{w_o}{w_o - 1}\right]^{\bar{q}'} \left[\frac{\bar{w}_o}{\bar{w}_o - 1}\right]^{q'} \left[2F_1 + \frac{N'}{\cos\gamma}(\rho_1 + 2\cos\gamma)F_2\right] , \tag{38b}$$

where now

$$F_i = F\left(-q', -\bar{q}'; 1; \frac{1}{|w_o|^2}\right) .$$

Equations (38) are the exact solution of the potential boundary value problem given by Eq. (35).

b. Application to the Through Flow

Before the types of approximations to be made are discussed it is illustrative to show the applicability of Eqs. (38) by using them to obtain the solution for the through flow of an impeller with logarithmic spiral blades.

If in the z-plane there is a source flow issuing from the origin at an angle α_1 to the radius, the velocity along a streamline can be shown to be

$$\frac{NQ}{2\pi r} \frac{1}{\cos\alpha_1} .$$

This velocity has a component $-V_n$ normal to the blade, and in order to make the blade a streamline, a flow must be added which has a component V_n that will cancel the contribution from the source. If γ is the angle of the blade to a radius then this component is

$$V_n = \frac{NQ}{2\pi r} \frac{\sin(\gamma - a_1)}{\cos a_1} .$$

By inspection of Eq. 35 it is seen that $m = -2$ and that

$$k = \frac{NQ}{2\pi\omega} \frac{\sin(\gamma - a_1)}{\cos\gamma \cos a_1} .$$

Upon substitution of these values into Eq. (38) one obtains

$$V_2 = -\frac{Q}{2\pi} C_H \frac{\sin(\gamma - a_1)}{\cos\gamma \cos a_1}$$

which is the same as that given by Eq. (15a) (except in slightly different form) for the tangential velocity at the point $w = 1$.

Boundary condition for nonlogarithmic spiral

Let us first consider a log-spiral blade of constant angle γ. If there is a source flow at the origin in the physical plane given by the potential

$$\frac{NQ}{2\pi} (1 - i \tan a_1) \log z ,$$

then the velocity component parallel to the blade is

$$V = \frac{NQ}{2\pi r} \frac{\cos(\gamma - a_1)}{\cos a_1} . \qquad (39)$$

This flow component is everywhere parallel to the blade surfaces, and the required solution is given correctly by Eqs. (15). Suppose, however, the blade angle is locally slightly different from γ (Fig. 10). The condition of no flow through the surface is then that

$$V_n' = V \tan \epsilon \qquad (40)$$

where V_n' is the perturbation velocity normal to the skeleton line of angle γ, V is given by the above and ϵ is the angular difference

$$\epsilon = \gamma' - \gamma , \tag{41}$$

γ' being the angle of the perturbed blade. It will now be assumed as is customary in thin airfoil theory, that boundary condition Eq. (40) may be applied on the logarithmic spiral. For simplicity it will also be assumed that $\epsilon \ll 1$ so that $\tan \epsilon = \epsilon$. With these assumptions the boundary condition on the logarithmic spiral may be expressed as

$$V_n' = \frac{N\Omega}{2\pi r} \epsilon \frac{\cos(\gamma - a_1)}{\cos a_1} . \tag{42}$$

If the angular perturbation ϵ is expressed as a power series in the radius the required solution can be readily obtained by means of Eqs. (38).

The present interest in this work is for pumping configurations and the function $\epsilon(r)$ will accordingly be specialized to suit this end. For this purpose it is convenient to express ϵ in terms of the circumferential variation y (Fig. 10). From the figure,

$$\theta' = \theta - y/r ,$$

and

$$\tan \gamma' = r \frac{d\theta'}{dr} .$$

Thus

$$\tan \gamma' = \tan \gamma \left[1 - \cot \gamma \frac{dy}{dr} + \frac{y}{r} \cot \gamma \right] .$$

Now if $\epsilon \ll 1$

$$\tan \gamma' = \tan \gamma + \epsilon / \cos^2 \gamma ,$$

then

$$\epsilon = \cos^2 \gamma \left[\frac{y}{r} - \frac{dy}{dr} \right] . \tag{43}$$

The variation y is useful in laying out impeller blade designs. The true length of the blade is customarily developed by graphical procedures, and typical blade variations are shown in Fig. 11 where it is seen that most

of the departure from a logarithmic-spiral occurs in the inlet regions. This fact is also important because it means that the blade shape perturbations are mainly subjected to the oncoming inlet flow. Hence for this reason the perturbation boundary conditions are based upon the component of the inlet flow parallel to the angle γ. This situation is different from cascade theory in which the vector mean of the inlet and outlet velocities is used.

Perturbations representative of pump design are

$$y = \lambda (1 - r)^3 \tag{44}$$

and

$$\frac{dy}{dr} = -3\lambda(1 - r)^2 ,$$

so that according to Eq. 43

$$\epsilon = \lambda \cos^2\gamma \left(\frac{1}{r} - 3r + 2r^2\right) . \tag{45}$$

The coefficient λ is determined by specifying ϵ at the inlet (since $\epsilon = 0$ at $r = 1$).

The equation for the boundary condition now reads

$$V_n' = \frac{NQ}{2\pi} \frac{\cos(\gamma - a_1)}{\cos a_1} \lambda \cos^2\gamma \left[\frac{1}{r^2} - 3 + 2r\right] . \tag{46}$$

The constants k and m in Eq. (35) can now be identified for the three terms of Eq. (46)

$$\left.\begin{aligned} k_1 &= \left(\frac{NQ}{2\pi\omega}\right) \frac{\cos(\gamma - a_1)}{\cos a_1} \lambda \cos\gamma ; \quad m = -3; \quad N' = -2N \\ k_2 &= -3 \left(\frac{NQ}{2\pi\omega}\right) \frac{\cos(\gamma - a_1)}{\cos a_1} \lambda \cos\gamma ; \quad m = -1; \quad N' = 2N \\ k_3 &= 2 \left(\frac{NQ}{2\pi\omega}\right) \frac{\cos(\gamma - a_1)}{\cos a_1} \lambda \cos\gamma ; \quad m = 0; \quad N' = N \end{aligned}\right\} . \tag{47}$$

With the aid of Eq. (38), each of the contributions of Eq. (47) to the tangential

velocity V_t' may be determined. They are:

$$V'_{t_2} = -\lambda \frac{\Omega}{\pi} \frac{\cos(\gamma - a_1)}{\cos a_1} \cos^2\gamma \left\{ J(-2N) \left[\frac{F_1(-2N) + 2N F_2(-2N)}{\rho_2} - \frac{2N F_2(-2N)}{2\cos\gamma} \right] \right.$$

$$- 3 J(2N) \left[\frac{F_1(2N) - 2N F_2(2N)}{\rho_2} + \frac{2N}{2\cos\gamma} F_2(2N) \right]$$

$$\left. + 2 J(N) \left[\frac{F_1(N) - N F_2(N)}{\rho_2} + \frac{N}{2\cos\gamma} F_2(N) \right] \right\} \quad . \qquad (48a)$$

and

$$V'_{t_1} = \lambda \frac{\Omega}{\pi} \frac{\cos(\gamma - a_1)}{\cos a_1} \cos^2\gamma \left\{ J(-2N) \left[\frac{F_1(-2N) + 2N F_2(-2N)}{\rho_1} + \frac{2N}{2\cos\gamma} F_2(-2N) \right] \right.$$

$$- 3 J(2N) \left[\frac{F_1(2N) - 2N F_2(2N)}{\rho_1} - \frac{2N}{2\cos\gamma} F_2(2N) \right]$$

$$\left. + 2 J(N) \left[\frac{F_1(N) - N F_2(N)}{\rho_i} - \frac{N}{2\cos\gamma} F_2(N) \right] \right\} \qquad (48b)$$

in which the special notation

$$J(N) = \left[\frac{w_o}{w_o - 1} \right]^{\bar{\eta}} \left[\frac{\bar{w}_o}{\bar{w}_o - 1} \right]^{q}$$

has been introduced. These equations may be evaluated by means of Eqs. (24) and in the case of $\sigma/2\pi > 1.2$ further simplification can be made.

The through flow solution then consists of the above correction terms plus the main contribution from the log-spiral solution. In like manner, correction terms for the displacement flow will be obtained.

c. Application to the Displacement Flow

The boundary condition on the perturbed blade is

$$V_n = r\omega \cos \gamma' = r\omega \cos(\gamma + \epsilon) .$$

The parameter ϵ is again supposed to be small compared to unity, and as in the preceding section this boundary condition is applied on the logarithmic spiral of γ = const. With these assumptions

$$V_n = r\omega \cos \gamma - \epsilon\, r\omega \sin \gamma$$

is the condition to be satisfied on the blade surface. However, the first term consists of the displacement flow already solved, the second term thus corresponds to the perturbation which accounts for the non-uniform angle, hence

$$V_n' = - r\omega\, \epsilon \sin \gamma \tag{49}$$

is the additional term which must be determined. If the specialized shape for pump blading is used (Eq.(44)) one obtains finally:

$$V_n' = - \lambda\, \omega \sin\gamma \cos^2\gamma \left[1 - 3r^2 + 2r^3\right] . \tag{50}$$

The constants k and N' are

$$\left.\begin{aligned} k_1 &= - \lambda \sin\gamma\cos\gamma \; ; \; m = -1, \quad N' = 2N \\ k_2 &= 3\lambda \sin\gamma \cos\gamma \; ; \; m = 1, \quad N' = \frac{2N}{3} \\ k_3 &= - 2\lambda \sin\gamma \cos\gamma \; ; \; m = 2, \quad N' = \frac{N}{2} \end{aligned}\right\} \tag{51}$$

The additional tangential velocity contributions are again found by use of Eqs. (38) to be

$$\begin{aligned} V_{d_2}' = -2\,\frac{\omega\lambda \sin\gamma \cos^2\gamma}{N} \Bigg\{ & -J(2N)\left[\frac{F_1(2N) - 2N\,F_2(2N)}{\rho_2} + \frac{2N}{2\cos\gamma}\,F_2(2N)\right] \\ & + 3J\left(\frac{2N}{3}\right)\left[\frac{F_1(2N/3) - 2N/3\,F_2(2N/3)}{\rho_2} + \frac{2N/3}{2\cos\gamma}\,F_2(2N/3)\right] \\ & - 2J\left(\frac{N}{2}\right)\left[\frac{F_1(N/2) - N/2\,F_2(N/2)}{\rho_2} + \frac{N/2}{2\cos\gamma}\,F_2(N/2)\right]\Bigg\} \end{aligned} \tag{52a}$$

and

$$V_{d_1}' = \frac{2\cos\lambda \sin\gamma\cos^2\gamma}{N} \left\{ - J(2N) \left[\frac{F_1(2N) - 2N F_2(2N)}{\rho_1} - \frac{2N}{2\cos\gamma} F_2(2N) \right] \right.$$

$$+ 3J(\tfrac{2N}{3}) \left[\frac{F_1(2N/3) - 2N/3\, F_2(2N/3)}{\rho_1} - \frac{2N/3\, F_2(2N/3)}{2\cos\gamma} \right]$$

$$\left. - 2J(\tfrac{N}{2}) \left[\frac{F_1(N/2) - N/2\, F_2(N/2)}{\rho_1} - \frac{N/2\, F_2(N/2)}{2\cos\gamma} \right] \right\} . \qquad (52b)$$

The effect of these perturbations on the head flow-rate equation will now be considered.

d. Head Flow-Rate Equation

From Section III the dimensionless head coefficient is seen to be

$$\psi = - \frac{N}{\omega} (V_{d_2} + V_{t_2} + V_{d_2}' + V_{t_2}')$$

where the primed quantities refer to the correction terms given by Eqs. (48) and (52). In order to evaluate these expressions the condition $\sigma/2\pi > 1.2$ will be imposed. Then if

$$\psi_o = 2\cos\gamma\ J(N) \left[\frac{F_1(N) - N F_2(N)}{\rho_2} + \frac{N}{\cos\gamma} F_2(N) \right] ,$$

$$\psi_o(-2N) \approx 1/\psi_o(2N) .$$

With these simplifications the head equation becomes

$$\psi = \psi_o + \psi_o' + \phi C_H(\tan\gamma - \tan\alpha_1) \left\{ 1 + \lambda \cot(\gamma - \alpha_1)\cos^2\gamma \right.$$

$$\left. \left[\frac{1}{\psi_o(2N)} + 2\psi_o(N) - 3\psi_o(2N) \right] \right\} \qquad (53)$$

where

$$\psi_o' = \lambda \sin\gamma\cos\gamma \left[3\psi_o(\tfrac{2N}{3}) - \psi_o(2N) - 2\psi_o(\tfrac{N}{2}) \right] . \qquad (54)$$

Equations (53) and (54) represent approximations which can be made if the solidity is sufficiently high. For the terms $\psi_o(2N)$ the approximations are satisfactory but are less accurate for $\psi(N/2)$. Although more accurate formulas may be obtained with the use of Eqs. (24), the present results provide a first-order correction to the head flow-rate equation.

These corrections are applicable for pumping configurations in which the major blade shape variations occur in the inlet portions of the impeller. It has already been stated that the shut-off coefficient ψ_o and the guiding parameter C_H are very insensitive functions of the solidity if it exceeds unity. Consequently, as a result of inlet perturbations one should expect only negligible changes in performance. Such indeed is the case in Eq. (54) since the ψ_o terms are all of the same order of magnitude and hence almost cancel each other. Thus changes in inlet angle should not result in significant performance changes. However, there should be a change in the shockless entry condition at least of the same order of magnitude as the variation of the inlet angle itself.

e. Shockless Entry

The additional contributions of Eqs. (48) and (52) are used in the same way as the development leading to Eq. (28a). Thus the condition for shockless entry is

$$(V_{t_1} - V_{t_2}) + (V_{d_1} - V_{d_2}) + (V_{t_1}' - V_{t_2}') + (V_{d_1}' - V_{d_2}') = 0 .$$

If the same approximations are to be made herein as in Eq. (54), then one may use the result

$$J(pN)\left[F_1(pN) - pN\,F_2(pN)\right] = \left[1 + \frac{8\pi^2\cos^2\gamma}{6p^2N^2}\right]\frac{1}{\psi_o(pN)}\left[\frac{r_1}{r_2}\right]^{2/p} .$$

The shockless entry condition then takes the form

$$\frac{\varphi_e'}{\varphi_e} = \frac{1+B}{1+A} \qquad (55a)$$

where

$$A = \lambda \cot(\gamma - \alpha_1)\cos^2\gamma \left\{ \left[\frac{r_2}{r_1} \right] \psi_o(2N) - \frac{3(r_1/r_2)}{\psi_o(2N)} + \frac{2(r_1/r_2)^2}{\psi_o(N)} \cdot \left[1 + \frac{8\pi^2 \cos^2\gamma}{6N^2} \right] \right\} \qquad (55b)$$

$$B = \frac{\lambda \cos\gamma \sin\gamma \ \psi_o(N)}{1 + \frac{8\pi^2\cos^2\gamma}{6N^2}} \left\{ \frac{3(r_1/r_2)}{\psi_o(2N/3)} \left[1 + \frac{3\pi^2\cos^2\gamma}{N^2} \right] - \frac{(r_2/r_1)}{\psi_o(2N)} - \frac{2(r_1/r_2)^2}{\psi_o(N/2)} \left[1 + \frac{16\pi^2\cos^2\gamma}{3N^2} \right] \right\} . \qquad (55c)$$

The ratio φ_e'/φ_e is the ratio of flow rates for shockless entry with and without the inlet angle perturbation. A close inspection of Eqs. (55b, c) shows that

$$\varphi_e'/\varphi_e < 1 \quad \text{for } \lambda > 0$$

$$\varphi_e'/\varphi_e > 1 \quad \text{for } \lambda < 0 .$$

This behavior is to be expected since if $\lambda > 0$, $\gamma' > \gamma$ and a "flatter" blade inlet angle results. This can be easily seen if the limiting case $N \to \infty$ is considered, since then

$$A \to \lambda \cot(\gamma - \alpha_1)\cos^2\gamma \left[\frac{r_2}{r_1} - 3\frac{r_1}{r_2} + 2\left(\frac{r_1}{r_2}\right)^2 \right] .$$

$$B \to \lambda \cos\gamma \sin\gamma \left[3\frac{r_1}{r_2} - \frac{r_2}{r_1} - 2\left(\frac{r_1}{r_2}\right)^2 \right] .$$

Presumably,

$$A, B << 1 \text{ so that}$$

$$\frac{\varphi_e'}{\varphi_e} = 1 + B - A .$$

With this simplification

$$\frac{\varphi_e'}{\varphi_e} = 1 - \frac{\epsilon}{\cos^2\gamma(\tan\gamma - \tan\alpha_1)} = \frac{\tan\gamma - \tan\alpha_1}{\tan(\gamma + \epsilon) - \tan\alpha_1}$$

which is the simple infinite vane theory. Equations (55) give the correct limiting value for shockless entry, but this result may be used as a "rule of thumb" for determining the flow rate for this condition. More exact values for a finite number of blades can, of course, be computed.

VII. Extension to Nonradial Profiles

Of particular interest to the designer, is the so-called "mixed-flow" impeller in which the flow approaches axially and progresses through the impeller on more or less conical surfaces. In certain cases it is possible to apply the results of the foregoing calculations to such impeller geometries and thereby obtain information in this important field of application.

The principal difficulty in such mixed flows is that the stream function and velocity potential both do not satisfy Laplace's equation, so that the methods of complex variables cannot be used. This circumstance is shown below in Eqs. (56) which are the equations to be satisfied by the velocity potential Φ and stream function Ψ for incompressible, perfect fluid flow over a conical surface with varying breadth b and constant vortex angle ζ i.e.,

$$\left.\begin{aligned} \frac{1}{R}\frac{\partial}{\partial R}\left[R\,b\,\frac{\partial\Phi}{\partial R}\right] + \frac{1}{R^2}\frac{\partial}{\partial\varphi}\left[b\,\frac{\partial\Phi}{\partial\varphi}\right] &= 0 \\ \frac{1}{R}\frac{\partial}{\partial R}\left[\frac{R}{b}\frac{\partial\Psi}{\partial R}\right] + \frac{1}{R^2}\frac{\partial}{\partial\varphi}\left[\frac{1}{b}\frac{\partial\Psi}{\partial\varphi}\right] &= 0 \end{aligned}\right\} \qquad (56)$$

The coordinate system is shown in Fig. 12. In the derivation of these equations it has been assumed that the curvature of the wall is small so that variations across the passage breadth may be neglected.

It is clear from Eq. (56) that if the breadth b is not constant then Φ and Ψ both do not satisfy Laplace's equation. However, an important deduction concerning the special case b = constant can be made.

a. Flow over a Conical Surface of Small Constant Breadth

If b is constant and if there are no variations across the breadth then Eqs. (56) reduce to Laplace's equation in the conical coordinates R, ω, and the two-dimensional calculations may be applied as follows: First, it is clear that if there are N blades, that the flow on the conical surface is periodic with a period of $2\pi \sin \zeta / N$. Thus if there are N blades on the cone, they are equivalent to $N/\sin \zeta$ in a straight radial array, i.e.

$$N^* = N/\sin \zeta . \tag{57a}$$

The other geometric properties of the array follow in a similar fashion. The radius ratio $R_2/R_1 = r_2/r_1$ remains unchanged. The solidity parameter becomes

$$\frac{\sigma^*}{2\pi} = \frac{N \log r_2/r_1}{2\pi \sin \zeta \cos \gamma} . \tag{57b}$$

The boundary conditions for the displacement and through flows are also the same as for the pure radial flow. This result is easily shown, for on the conical surface

$$V_n = \bar{\omega} \times \bar{R} \cos \gamma = R \omega \sin \zeta \cos \gamma = r \omega \cos \gamma .$$

Hence, the radial flow calculations may be applied to the flow in a conical impeller of constant breadth if the equivalent number of radial blades is given by Eq. (57a) and the solidity by Eq. (57b).

An interesting limiting case is provided by making $\zeta \to 0$ but keeping σ^* constant.

If $R_2 - R_1$ is the slant blade height then

$$\frac{\sigma^*}{2\pi} \to \frac{N \log \left(1 + \frac{R_2 - R_1}{R_1}\right)}{2\pi \sin \zeta \cos \gamma}$$

and as $\zeta \to 0$ and $R_2 \sin \zeta = r_2$ is a constant, one obtains

$$\frac{\sigma^*}{2\pi} = \frac{N(R_2 - R_1)}{2\pi r_2 \cos \gamma}$$

which is the definition of solidity for a two-dimensional cascade. The flow coefficients of the radial case also become equal to the cascade results since if σ^* is constant and $N/\sin \zeta \to \infty$ then the head coefficient (Eq. (25a)) becomes

$$\psi_o = C_H$$

which is the cascade result.

b. Effect of Variation in Breadth

From the foregoing discussion it is evident that a realistic treatment of the effect of breadth variation cannot be done by complex variable methods. However, if db/dR is small compared to unity then approximations based on complex variable methods should give correction terms of the right magnitude and in the limiting case of an infinite number of vanes, converge to the exact answer.

For the sake of simplicity, in this section it will be assumed that $\zeta = 90^\circ$, i.e., a straight radial impeller. In Section V-b, the through flow solution was obtained by computing the "interference" velocity necessary to make the blade a streamline, and using this velocity component as a boundary condition in Eqs. (38). Now it is clear that if the breadth is varied, the interference velocity will be changed and hence a different flow will result. In this section the additional terms for the through flow will be worked out. Inasmuch as the displacement flow boundary condition is independent of the breadth, no additional correction terms should be expected to occur,

The boundary condition

$$V_n = \frac{NQ}{2\pi r} \frac{\sin(\gamma' - a_1)}{\cos a_1} \frac{b_2}{b(r)} \qquad (57)$$

applied along the blade surface makes it a streamline in the through flow where b_2 and $b(r)$ are the impeller widths at the exit and at any radius r respectively, and γ' is the angle of the perturbed blade as before. The restriction $\epsilon = \gamma' - \gamma << 1$ will be retained so that

$$\sin(\gamma' - a_1) = \sin(\gamma - a_1) + \epsilon \cos(\gamma - a_1) ,$$

and if the breadth term be written as

$$b_2/b(r) = 1 + f(r) \tag{58}$$

the boundary condition becomes:

$$V_n = \frac{NQ \sin(\gamma - a_1)}{2\pi r \cos a_1} + \frac{NQ \sin(\gamma - a_1)}{2\pi r \cos a_1} f(r) + \epsilon \frac{NQ \cos(\gamma - a_1)}{2\pi r \cos a_1} \left[1 + f(r)\right] .$$

The first and third term of this expression have already been worked out in Sections III and V-b respectively. Thus the additional term required for breadth variation is

$$V_n'' = \frac{NQ \sin(\gamma - a_1)}{2\pi r \cos a_1} f(r) \left[1 + \epsilon \cot(\gamma - a_1)\right] . \tag{59a}$$

In keeping with the spirit of the foregoing approximations, ϵ will be neglected compared to unity. It should be pointed out that this assumption results in a linear theory. In order to obtain the solution of Eq. (59) by means of Eq. (38) the function $f(r)$ must be expressed in a power series. Although any particular function could be worked out, it seems most to the point to evaluate the effect of breadth variation for the simplest case possible, namely, a linear one. For some mixed flow designs this is a fairly realistic choice but Francis type impellers require more complicated functions. Thus, assume

$$f(r) = \mu(1 - r) , \tag{60}$$

so that

$$V_n'' = \mu \frac{NQ \sin(\gamma - a_1)}{2\pi \cos a_1} \left(\frac{1}{r} - 1\right) \tag{59b}$$

In terms of Eq. (35) one has

$$k_1 = \mu \frac{NQ \sin(\gamma - a_1)}{2\pi \omega \cos a_1 \cos \gamma} \; ; \quad m = -2, \quad N' = \infty$$

$$k_2 = -\mu \frac{NQ \sin(\gamma - a_1)}{2\pi \omega \cos a_1 \cos \gamma} \; ; \quad m = -1, \quad N' = 2N$$

hence the perturbation tangential velocities (found from Eq. (35)) are

$$\left.\begin{aligned} V_{t_2}'' &= -\mu \frac{Q \sin(\gamma - a_1)}{\pi \cos a_1} \left[J(2N) \left\{ \frac{F_1(2N) - 2N F_2(2N)}{\rho_2} + \frac{2N}{2 \cos \gamma} F_2(2N) \right\} - \frac{1}{\rho_2} \right] \\ \text{and} \\ V_{t_1}'' &= \mu \frac{Q \sin(\gamma - a_1)}{\pi \cos a_1} \left[J(2N) \left\{ \frac{F_1(2N) - 2N F_2(2N)}{\rho_1} - \frac{2N}{2 \cos \gamma} F_2(2N) \right\} - \frac{1}{\rho_1} \right] \end{aligned}\right\} \quad (61)$$

These results may be used in conjunction with Eqs. (48) and (52) to obtain correction terms to the head flow-rate equation. However, one may expect these terms to be small for pumping configurations and also that the only major change will be in the condition for smooth entry.

With the former restrictions on the solidity one has approximately

$$V_{t_1}'' - V_{t_2}'' = \mu \frac{Q \sin(\gamma - a_1)}{\pi \cos a_1} \left[\frac{r_1}{r_2} \frac{1}{\psi_o(2N)} - 1 \right] \left[\frac{1}{\rho_1} + \frac{1}{\rho_2} \right] .$$

When this expression is included in the shockless entry condition Eq. (55a) remains unchanged except that A is replaced by A', i.e.,

$$\frac{\varphi_e''}{\varphi_e} = \frac{1 + B}{1 + A'} , \quad (60a)$$

or

$$\frac{\varphi_e''}{\varphi_{e'}} = \frac{1 + A}{1 + A'} \quad (60b)$$

where

$$A' = A + \mu \left[\frac{r_1}{r_2} \frac{1}{\psi_0(2N)} - 1 \right] , \tag{61}$$

and φ_e'' is the flow rate coefficient for shockless entry for an impeller with variable breadth and nonconstant blade angle. The coefficient A is given by Eq. (55b).

If $\mu > 0$, the impeller inlet is smaller than the exit (Eq. (60)), so that the shockless flow rate must decrease (Eq. (60b)). However, the usual case is that the inlet breadth is greater than that of the exit so that $\mu < 0$ and the ratio

$$\frac{\varphi_e''}{\varphi_e'} > 1$$

In the limit $N \to \infty$, Eq. (60b) becomes

$$\frac{\varphi_e''}{\varphi_e'} = \frac{b_2}{b_1} \tag{62}$$

which is precisely the result of the infinite vane theory. If there is no prewhirl ($\alpha_1 = 0$) this limiting condition can also be written as

$$\frac{\tan \gamma_1}{\tan \gamma_2} = \frac{b_2}{b_1}$$

where now γ is the relative flow angle at the inlet for two different breadths. Both this equation and Eq. (62) are really the conditions for maintaining the same incidence angle to the blade inlet. Without undertaking detailed calculations this result is probably as good a rule as any other for inlet breadth variation.

More complicated breadth variations could be used to account for different profile shapes. However, it is doubtful whether or not they will add significantly to the results of Eq. (60) in view of the already approximate nature of the solution. In fact because of the obvious crudeness of the breadth approximations we have been somewhat hesitant to present them, and have done so only because we are unable to find similar computations elsewhere.

c. Remark on Application to Mixed Flow Impellers

With the aid of the theory developed thus far it is possible to make more extended analytic computations of mixed flow impeller performance than heretofore possible. Thus far, the effect of the blade forces on the meridional streamline distribution have been neglected. In the case of radial or mixed flow pumps the deviations can probably be overlooked at least at the design point unless blades of unusually high "warp" are employed or if the total head distribution is not uniform across the passage at the design point. In any case, these effects may be approximately calculated by theories recently made available.[16, 17]

For most conventional designs with constant total head developed across the passage it will still be necessary to obtain the meridional streamline and velocity distribution and thus work out a "pseudo-three-dimensional" solution by application of the foregoing theory to each stream lamina. The blade sections can then be designed to have smooth entry occur simultaneously across the inlet or any other condition.

This discussion will be closed by observing that although the present theory is applicable for the straight radial or conical profiles it is still inadequate for the smooth entry calculations of Francis type impellers with rather large meridion curvatures. In this situation the flow may be imagined to take place on an infinitesimally thin lamina of revolution and the methods of conformal mapping can be applied to this "two-dimensional" problem.[18]

d. Remark on the Influence of Compressibility

A general treatment of the radial flow turbomachine problem is too difficult to be attempted directly. Specific cases have been worked out numerically[1] for the pressure and velocity distributions in the passage. Radial flow compressor configurations in general have rather high values of the solidity, e.g., $\sigma/2\pi \geq 2$ are not uncommon. For these cases it seems reasonable to suppose that the design coefficients ψ_o and C_H will be little affected even for pressure ratios on the order of two or three since the relative velocities are still quite subsonic. That this is indeed the case is shown in Ref. 1 wherein the value of the coefficient ψ_o differs by less than one percent for an impeller operating with a tip Mach number of 1.5 and zero. In fact, the value of these coefficients for compressible flow is only about one percent

different from the results given in Fig. 6.

Thus, it would appear that for configurations of high solidity the incompressible calculations give a good approximation for compressible flow performance, except for the maximum mass flow which depends mainly upon the inlet design. The head flow-rate curve should then be nearly the same if the volume flow parameter is based on the exit volume, i.e.,

$$\phi = \frac{V_{2u}}{u_2} = \frac{m}{\rho_2 u_2}$$

where m is the mass flow-rate/exit area/sec and ρ_2 is the exit density. The total pressure ratio then becomes

$$\frac{P_2}{P_1} = \left\{ \frac{U_2^2}{c_p T_o g J} \left[\psi_o - \frac{C_H m (\tan\gamma - \tan\alpha_1)}{\rho_o \left(\frac{P_2}{P_1}\right)^{1/k} u_2} \right] + 1 \right\}^{\frac{k}{k-1}} \qquad (63)$$

where k is the ratio of specific heats, J the mechanical heat equivalent, ρ_o, T_o are the inlet density and static temperature respectively.

e. Numerical Examples

In this section a few examples illustrating the use of the graphs will be worked out.

1. Consider a radial flow pump of constant breadth with 6 blades of constant angle $\gamma = 70^\circ$, radius ratio 0.5, and with no pre-whirl, i.e., $\alpha_1 = 0$. The solidity is

$$\frac{\sigma}{2\pi} = 6 \ln 2/2\pi \cos\gamma = 1.94$$

so that Eqs. (25b) and (29) may be used safely. The shut-off coefficient is (Fig. 6) $\psi_o = 0.81$ and $C_H = 1.00$. Thus the head flow-rate relation (Eq. (20b)) for backward curved blades becomes

$$\psi = 0.81 - 2.745\phi ,$$

the condition for shockless entry is (Eq. (29))

$$\frac{\varphi_e}{\varphi_{e_\infty}} = \frac{1}{0.81}\left(1 + \frac{8\pi^2 \cos^2 70^\circ}{6 \times 36}\right) = 1.29$$

or 29% more than the simple theory would indicate. Now

$$\varphi_{e_\infty} = (r_1/r_2)^2 \cot \gamma = 0.091 \ ,$$

thus

$$\varphi_e = 0.117 \ .$$

Since there is no inlet whirl, the absolute exit flow angle α_2 is given by

$$\tan \alpha_2 = \psi/\varphi$$

or

$$\alpha_2 = 76^{1/2^\circ}$$

at the shockless flow rate.

It should be emphasized that ψ_o is only a parameter useful in determining that part of the head curve near the design point. Gross real fluid effects prevent ψ_o from being realized near shut-off.

2. If it is desired to operate the pump of Ex. 1 at a shockless flow rate of $\varphi = 0.100$, then the inlet angle γ_1 will have to be increased (i.e. made flatter). Thus from Eq. (55a)

$$\frac{\varphi_e'}{\varphi_e} = \frac{0.100}{0.117} = 0.855 \ .$$

Since γ , N, r_1/r_2 are known, λ in Eqs. (55b, c) can be found. For $\alpha_1 = 0$

$$A = 0.0324\,\lambda$$
$$B = -0.224\,\lambda$$

hence

$$\lambda = 0.566 \ .$$

By Eq. (45)

$$\epsilon = 0.0664 = 3.8^\circ$$

or $\gamma_i = 73.8^\circ$. The inlet angle must be increased by about 4° in order to have smooth entry occur at $\phi = 0.100$. At this operating condition the incidence angles to the blade is 5.5° whereas in the case of Ex. 1 it is 5° at shockless. For this case then, the simple rule of maintaining a constant angle of attack or incidence to the blade will satisfy the smooth entry condition. For smaller values of $\lambda/2\pi$, however, deviations from this rule must be expected to occur. Without further calculation we may also suppose that the same result holds true for minor breadth variations.

3. Let the pump of Ex. 1 be operated now as a normal turbine. In general there will be some whirl leaving the impeller so that $\alpha_1 \neq 0$. For the normal direction of operation Eqs. (30) and (32) give

$$\psi = \phi(2.75 - \tan\alpha_2) - 0.322 .$$

Typical values of α_2 are in the interval $-80^\circ \leq \alpha_2 \leq -60^\circ$. If the value of α_2 is chosen is that for the normal pump operation in Ex. 7, i.e., $\alpha_2 = -78.5^\circ$ then

$$\psi = 6.91\phi - 0.32$$

is the performance of the pump in Ex. 1 operated as a turbine. The condition of no exit whirl is the same as that of the shockless flow rate in Ex. 1, viz. $\phi = 0.117$.

4. In the last example a 70° angle pump with 5 blades, constructed on a 45° cone with a radius ratio of 0.7 will be considered. The solidity of this configuration is

$$\frac{\sigma^*}{2\pi} = \frac{N \ln r_2/r_1}{2\pi \sin\zeta \cos\gamma} = \frac{5 \ln 2}{2\pi \sin 45^\circ \cos 70^\circ} = 1.17$$

which is large enough for the approximations of Eq. (25b) and (29) to be used. The equivalent number of radial blades is $N^* = N/\sin\zeta = 7.1$, hence from Figs. 5 and 6

$$C_H = 0.983$$

$$\psi_o = 0.83 .$$

The coefficients ψ_o given in Fig. 6 are the maximum values for the given number of blades. Unless C_H falls several percent less than unity closer approximations of ψ_o do not have to be made. In that event, however, Eq. (25a) will provide a first order correction.

For $a_1 = 0$, the head equation is

$$\psi = 0.83 - 2.70\,\varphi ,$$

and shockless entry occurs at

$$\varphi_e = \varphi_{e\infty}\,\frac{1}{(0.83)}\left\{1 + \frac{4}{3}\left[\frac{\pi^2 \cos^2 70^\circ}{7.1}\right]^2\right\}$$

$$\varphi_e = 0.222 .$$

If the breadth of the impeller is comparable to the radius then the analysis will have to be done for a number of streamlines. It is customary to design pumps in such a way so as to have a constant head developed across the exit breadth. The meridian velocity distribution is then only slightly affected by the blade loading and one may use any means to obtain the meridian flow. However, at "off design" flows, the effect of the blade loading will become important for small values of ζ, i.e., shallow conical pumps, and recalculation of the meridian velocity profiles by the methods of Ref. 16 may become necessary.

VIII. Concluding Remarks

There have been three purposes in presenting this material. The first has been to outline an exact theory for potential flow in impellers with logarithmic spiral vanes. The second has been to describe an analytic "thin airfoil" theory which could account for the effect of blade angle variation. This approximate theory starts from the solution of the potential flow through a radial array of log-spiral blades with the normal velocity component being prescribed as any power function of the radius. A method is shown whereby these solutions may be used to obtain correction terms for small variations

in vane angle and passage breadth and also when the meridional streamlines are cones.

The last objective has been to develop the theory in a form suitable for radial flow pump and turbine configurations. Formulas and charts, useful for rapid performance estimates, are provided for this field subject to the restriction that the solidity be greater than about 1.2. However, general results are also given so that other designs may be determined.

It would have been desirable to include a number of detailed impeller computations in which account is taken of the meridional streamline distribution. The work involved is considerable, however, and for that reason such results are not presented here.

It would also be of interest to extend the present theory to account for the effect of strong meridional curvature (i.e. Francis type impellers). This would complete the theory of the "pseudo-three-dimensional" impeller with a finite number of blades. The writer is interested in this problem and would like to see examples of such calculations made available so that the importance of these parameters could be determined.

IX. Notation

List of Symbols

A - Area

F - Complex velocity potential, hypergeometric function as noted

N - Number of impeller blades

Q - Flow rate through one impeller passage

T - Torque

U - Circumferential velocity = $r\omega$

V - Absolute velocity

W - Relative velocity

C_H - Flow-rate correction factor

a - $|w_o|$

b - Breadth of impeller passage

g - Gravitational constant

k, m, n - Constants

r - Radius in physical plane

q - Complex constant

w - Complex coordinate in circle plane

w_o - A constant in the w-plane representing the origin of the z-plane = $ae^{i\delta}$

z - Complex coordinate in physical plane = $x + ig$

α - Angle between absolute flow and radius vector, (Positive increasing counter-clockwise)

γ - Angle between blade tangent and radius vector

δ - Argument of w_o

ϵ - Angular perturbation of blade

ζ - Cone angle

θ, ϖ - Angular coordinates

λ - Constant

ρ - Radius vector in w-plane

σ - Solidity = $\dfrac{V \ln r_2/r_1}{\cos \gamma}$

τ - Torque coefficient at constant speed = $\varphi\psi$

Φ - Velocity potential

φ - Flow-rate coefficient = $NQ/2\pi A_2 V_2 = V_{r_2}/V_2$

χ - Torque coefficient at constant flow-rate = ψ/φ

Notation (continued)

Ψ - Stream function

ψ - Head coefficient = $H/U_2^2/g$

ω - Angular speed

Superscripts

$\bar{}$ - Conjugate i.e., $z = x + iy$, $\bar{z} = x - iy$

$*$ - Conjugate function

Subscripts

b - refers to impeller blade quantities

d - displacement flow tangential velocity component

e - conditions at shockless or smooth entry

n - normal velocity component

r - radial velocity in w-plane

t - through flow tangential velocity component

z - velocity in z-plane

u - circumferential component of velocity in z-plane

w - velocity in w-plane

θ - tangential velocity in w-plane

Γ - circulation flow velocity component

o - conditions at no flow for a pump

oT - conditions at no flow for a turbine

1 - conditions at inlet

2 - conditions at exit

∞ - conditions based on an infinite number of vanes

X. References

1. Stanitz, John D., Ellis, Gaylord O., "Two-dimensional Flow on General Surfaces of Revolution in Turbomachines", NACA TN 2654.

2. Chung-Hua Wu, Brown, Curtis A., Prian, Vasily D., "An Approximate Method of Determining the Subsonic Flow in an Arbitrary Stream Filament of Revolution Cut by Arbitrary Turbomachine Blades", NACA TN 2702.

3. Spannhake, W., "Anwendung der conformen Abbildung auf die Berechnung von Strömungen in Kreiselrädern", ZAMM, Vol. 5, 1925, p. 481.

4. Sörensen, E., "Potential Flow Through Pumps and Turbines", NACA TN 973.

5. Busemann, A., "Das Förderhohenverhaltnis von Kreiselpumpen mit logarithmischspiraligen Schaufeln", ZAMM, Vol. 8, 1928.

6. Durand, W.F., "Aerodynamic Theory", Vol. II, Springer, Berlin, 1935, p. 71.

7. Milne-Thompson, L.M., "Theoretical Hydrodynamics", MacMillan, 1950, p. 149.

8. Wislicenus, G.F., "Fluid Mechanics of Turbomachinery", McGraw-Hill, 1947, p. 141.

9. Copson, E.T., "Theory of Functions of a Complex Variable", Oxford University Press, 1935, Ch. 10.

10. Dwight, H.B., "Tables of Integrals", MacMillan, 1947.

11. Acosta, A.J., "An Experimental and Theoretical Investigation of Two-dimensional Centrifugal Pump Impellers", Hydrodynamics Laboratory, California Institute of Technology Report No. 21-9.

12. Garrick, I.E., "On the Plane Potential Flow Past a Lattice of Arbitrary Airfoils", NACA Report No. 788.

13. Bowen, J.T., Sabersky, R.H., Rannie, W.D., "Theoretical and Experimental Investigations of Axial Flow Compressors", 1949, Mechanical Engineering Laboratory, California Institute of Technology.

14. Pistolesi, E., "On the Calculation of Flow Past an Infinite Screen of Thin Airfoils", NACA TM 968.

15. Betz, A., Flügge-Lotz, I., "Design of Centrifugal Impeller Blades", NACA TM 902.

References (continued)

16. Chung-Hua Wu, Brown, Curtis A., Costilow, Eleanor L., "Analysis of Flow in a Subsonic Mixed-Flow Impeller", NACA TN 2749.

17. Holmquist, Carl O., "An Approximate Method of Calculating Three-dimensional Compressible Flow in Axial Turbomachines", unpublished thesis 1953, California Institute of Technology.

18. Smythe, W.R., "Static and Dynamic Electricity", McGraw-Hill, 1939, p. 241

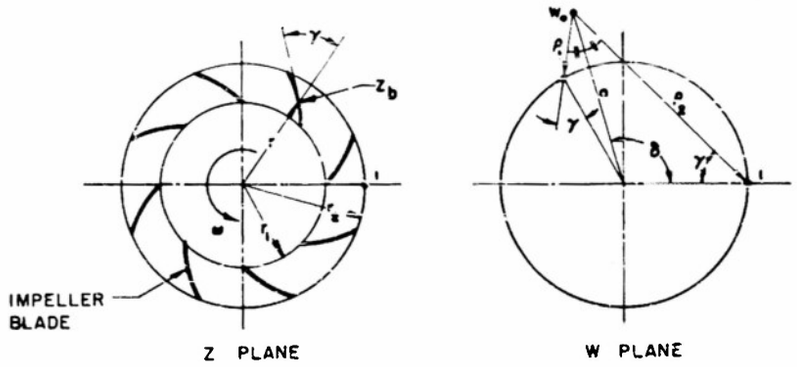

Fig. 1 - Sketch illustrating the mapping from the physical (z) plane to the circle (w) plane.

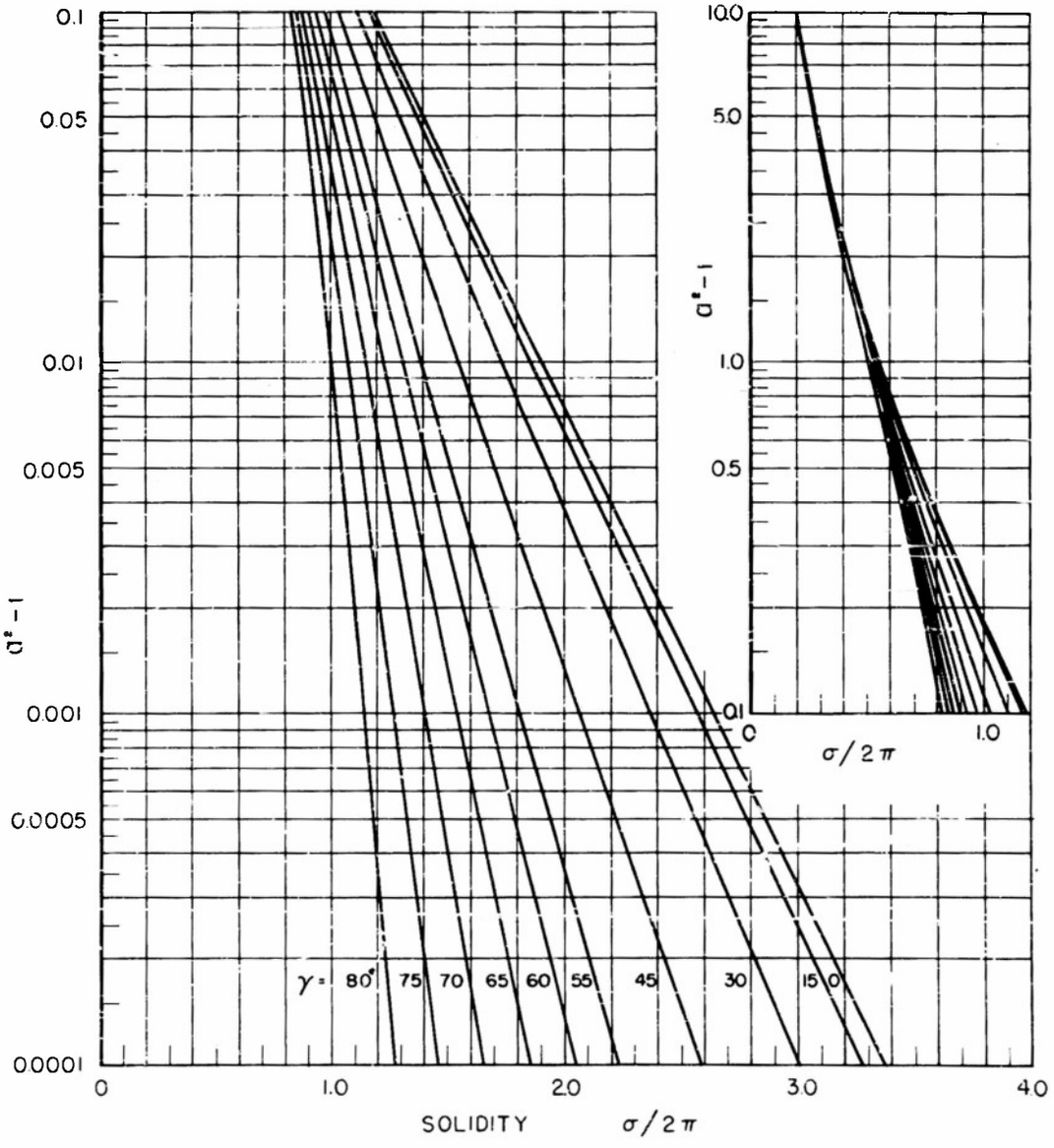

Fig. 2 - Values of the mapping parameter $a^2 - 1$ vs. the solidity $\sigma/2\pi = N \log_e r_2/r_1 / 2\pi \cos \gamma$.

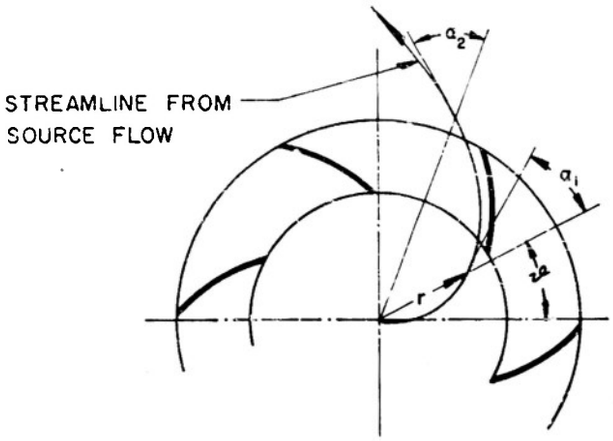

Fig. 3 - Definition sketch showing direction of positive α.

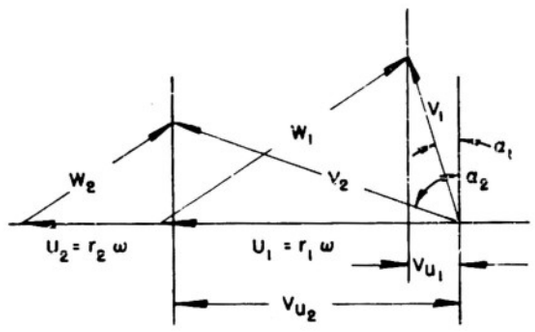

Fig. 4 - Definition sketch showing inlet and exit velocity triangles for backward curved vanes.

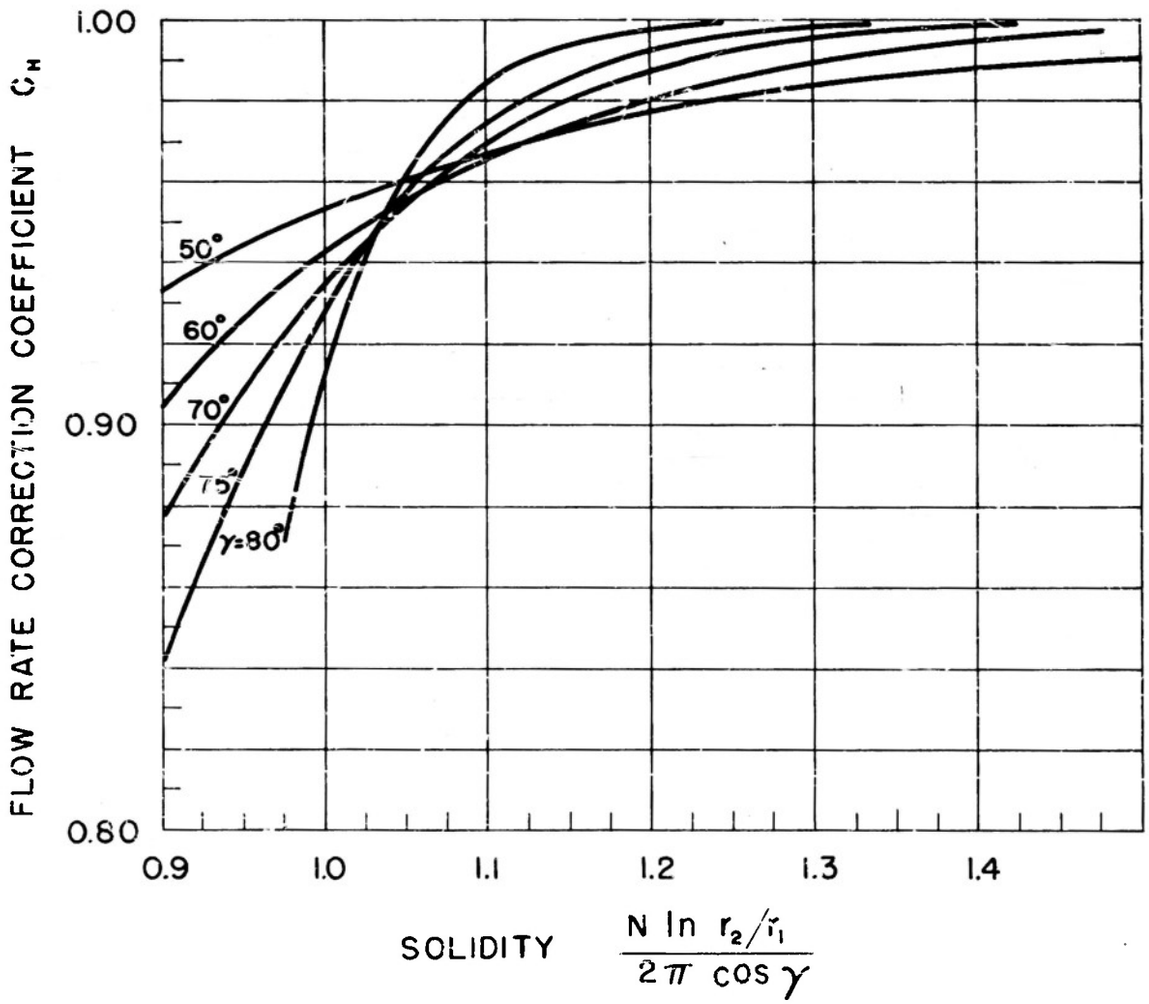

Fig. 5 - Correction factor C_H vs. solidity for various values of γ.

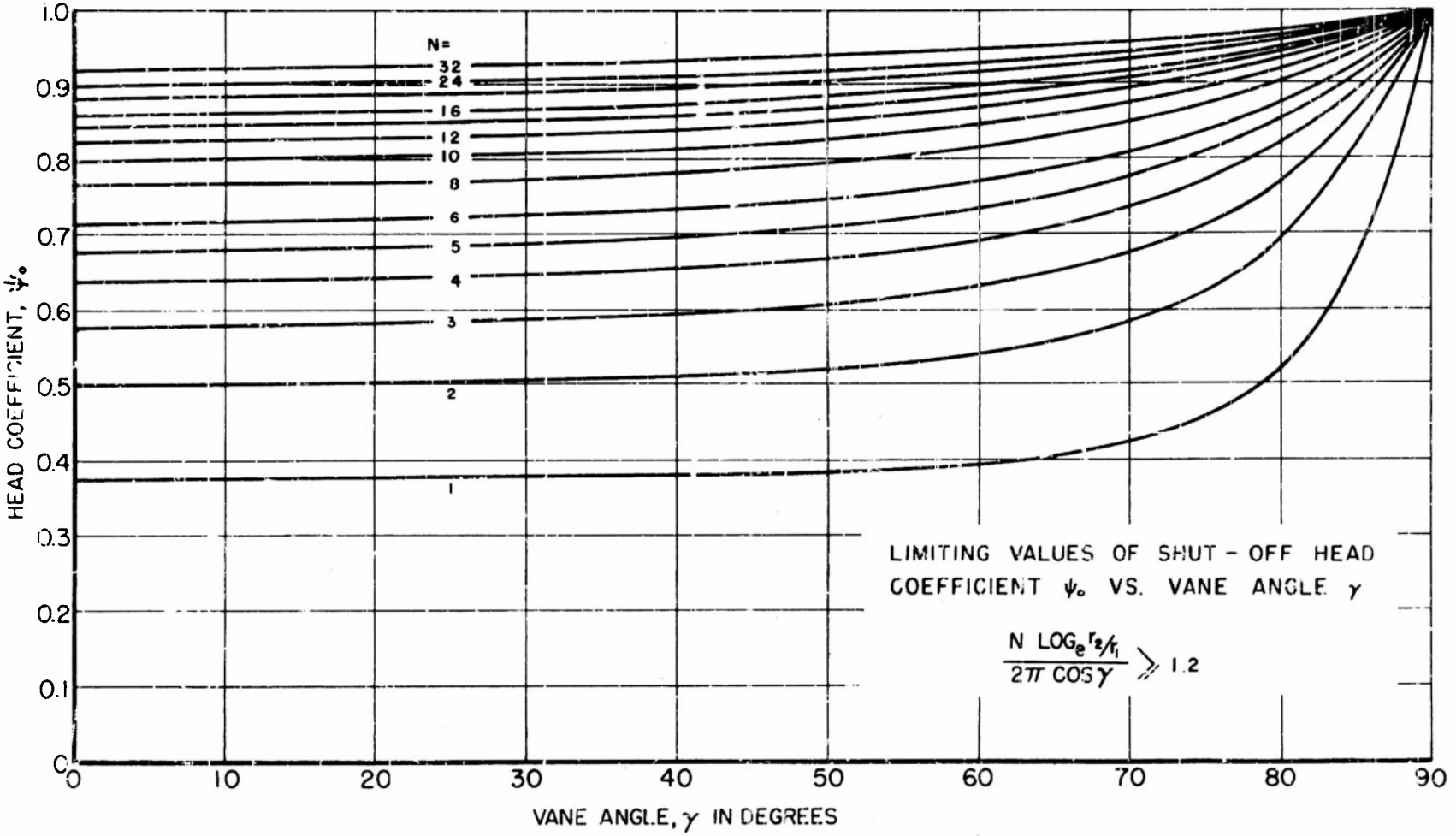

Fig. 6 - Limiting value of shut-off head coefficient ψ_o vs. stagger angle γ various values of N.

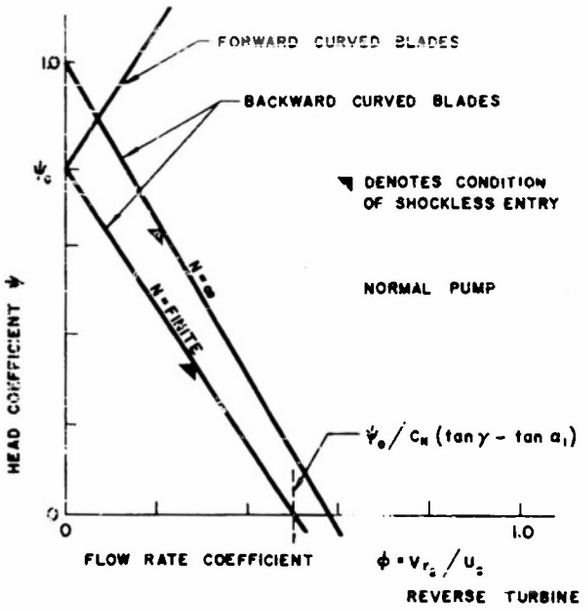

Fig. 7 - Head-flow rate characteristic line for a pump impeller operating in frictionless incompressible fluid with a finite number of blades.

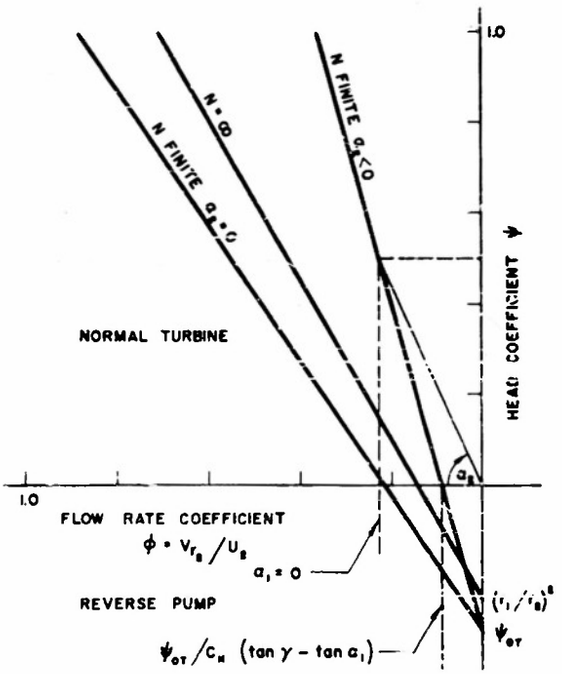

Fig. 8 - Theoretical head-flow rate characteristics for a turbine rotor with a finite number of blades operating at constant speed. Note that the flow coefficient axis is the negative of that for a pump.

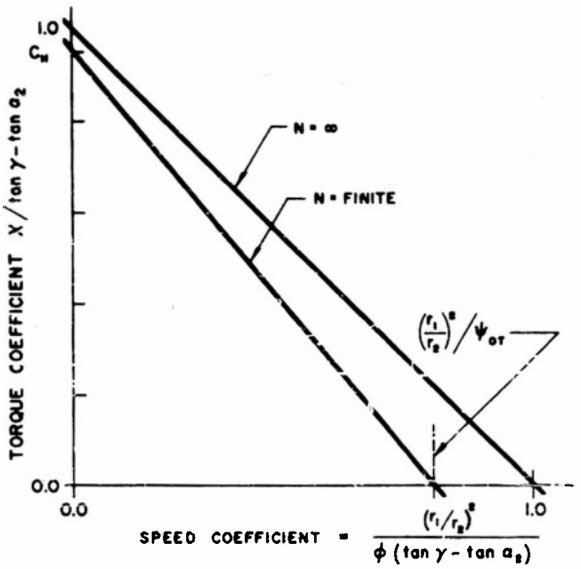

Fig. 9 - Theoretical torque coefficient vs. speed coefficient for a turbine operated at constant flow rate.

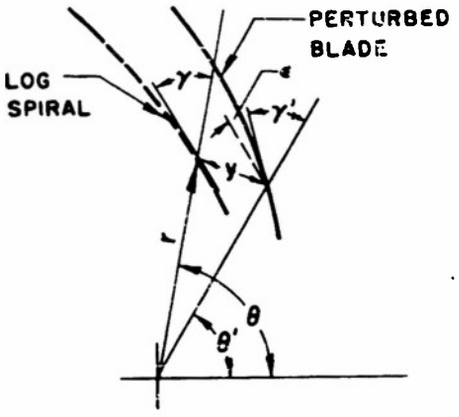

Fig. 10 - Sketch illustrating parameter for a perturbed blade shape.

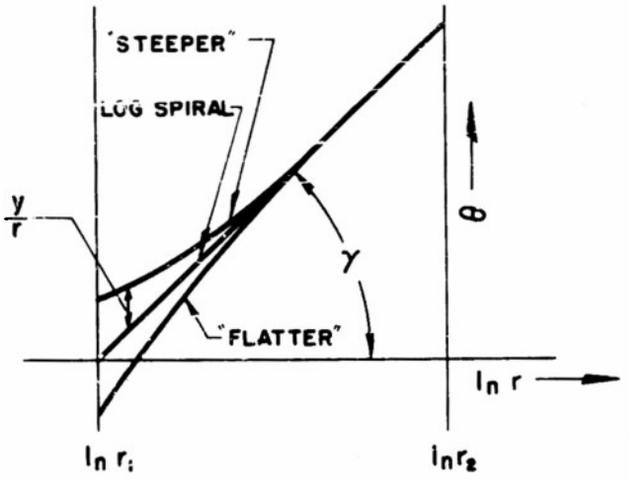

Fig. 11 - Sketch showing type of perturbations useful in pump designs. The plane shown is the logarithm of the physical or real plane.

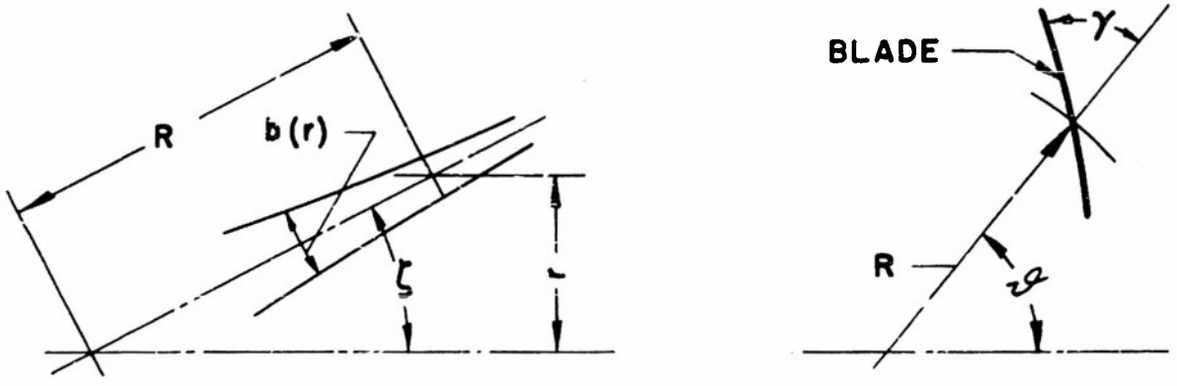

Fig. 12 - Definition sketch for mixed flow conical pump of variable breadth.

DISTRIBUTION LIST - CONTRACT N6onr-24402
Hydrodynamics Laboratory
California Institute of Technology

Chief of Naval Research
Department of the Navy
Washington 25, D.C.
Attn: Code 429 1
Code 438 2

Commanding Officer
Office of Naval Research
Branch Office
John Crerar Library Bldg.
86 E. Randolph Street
Chicago 1, Illinois 1

Commanding Officer
Office of Naval Research
Branch Office
346 Broadway
New York 13, New York 1

Commanding Officer
Office of Naval Research
Branch Office
1030 E. Green Street
Pasadena 1, California 2

Commanding Officer
Office of Naval Research
Branch Office
1000 Geary Street
San Francisco, California 1

Chief, Bureau of Aeronautics
Department of the Navy
Washington 25, D.C.
Attn: Research Division 1

Chief, Bureau of Ordnance
Dept. of the Navy
Washington 25, D.C.
Attn: Code Re6a 1
Research and Development
Division 1

Commanding Officer
Naval Ordnance Laboratory
White Oak, Silver Spring, Md. 1

Commander
Naval Ordnance Test Station
3202 E. Foothill Blvd.
Pasadena, California
Attn: Mr. J. Neustein 1

Commanding Officer
Naval Torpedo Station
Keyport, Washington 1

Chief, Bureau of Ships
Department of the Navy
Washington 25, D.C.
Attn: Research Div. 1
Prop and Shaft Branch 1

Documents Service Center
Armed Services Technical
Information Agency
Knott Building
Dayton 2, Ohio 5

Director
Naval Research Laboratory
Washington 20, D.C.
Attn: Code 2021 1

Commanding Officer and Director
David Taylor Model Basin
Washington 7, D.C.
Attn: Hydromechanics Lab. 1
Hydromechanics Div. 1
Ship Div. 1
Technical Library 1

Commanding General
Office of Ordnance Research
Department of the Army
Washington 25, D.C. 1

Directorate of Intelligence
Headquarters, U.S. Air Force
Washington 25, D.C.
Attn: Director, Research and
Development 1

Commanding General
Air Research and Development
Command
Office of Scientific Research
Post Office Box 1395
Baltimore 3, Maryland 1

Distribution List - Contract N6onr-24402 (continued)
Hydrodynamics Laboratory
California Institute of Technology

Director of Research
National Advisory Committee for Aeronautics
1724 F Street, Northwest
Washington, D.C.
Attn: Director of Research 1

Director
Langley Aeronautical Laboratory
National Advisory Committee for Aeronautics
Langley Field, Virginia 1

Director
Ames Aeronautical Laboratory
National Advisory Committee for Aeronautics
Moffett Field, California 1

Director
Lewis Flight Propulsion Laboratory
National Advisory Committee for Aeronautics
21000 Brookpark Road
Cleveland 11, Ohio 1

Director
National Bureau of Standards
National Hydraulic Laboratory
Washington 25, D.C.
Attn: Dr. G. B. Schubauer 1

Polytechnic Institute of Brooklyn
Dept. of Aeronautical Engineering and Applied Mechanics
99 Livingston Street
Brooklyn 2, New York
Attn: Professor A. Ferri 1
: Professor H. J. Reissner 1

Polytechnic Institute of Brooklyn
Dept. of Mechanical Engineering
99 Livingston Street
Brooklyn 2, New York
Attn: Professor C.H. Wu 1

The Johns Hopkins University
Dept. of Mechanical Engineering
Baltimore 18, Maryland
Attn: Dr. G. F. Wislicenus 1

Massachusetts Institute of Technology
Hydrodynamics Laboratory
Cambridge 39, Mass.
Attn: A. T. Ippen 1

Massachusetts Institute of Technology
Dept. of Naval Architecture
Cambridge 39, Mass. 1

Massachusetts Institute of Technology
Department of Mechanical Engineering
Cambridge 39, Mass.
Attn: Professor E. S. Taylor 1

Ordnance Research Laboratory
Pennsylvania State College
State College, Pennsylvania
Attn: Dr. J. M. Robertson 1

Princeton University
Department of Mechanical Engineering
Princeton, New Jersey
Attn: Professor C. P. Kittridge 1

State University of Iowa
Iowa Institute of Hydraulic Research
Iowa City, Iowa
Attn: Dr. Hunter Rouse, Director 1

Experimental Towing Tank
Stevens Institute of Technology
711 Hudson Street
Hoboken, New Jersey 1

University of California
Department of Mechanical Engineering
Los Angeles, California
Attn: Dr. H. A. Einstein 1

University of Maryland
Institute for Fluid Mechanics and Applied Mathematics
College Park, Maryland
Attn: Professor J. R. Weske 1

University of Minnesota
St. Anthony Falls Hydraulic Laboratory
Minneapolis 14, Minnesota
Attn: Dr. L. G. Straub 1

University of Notre Dame
College of Engineering
Notre Dame, Indiana
Attn: Dr. K. E. Schoenherr, Dean 1

Distribution List - Contract Nonr-24402 (continued)
Hydrodynamics Laboratory
California Institute of Technology

University of Tennessee
Engineering Experimental Station
Knoxville, Tennessee
Attn: Dr. G. H. Hickox
Associate Director 1

Worcester Polytechnic Institute
Alden Hydraulic Laboratory
Worcester, Mass.
Attn: Professor L. J. Hooper 1

Aerojet General Corporation
6352 Irwindale Avenue
Azusa, California
Attn: Mr. C. A. Gongwer 1

California Institute of Technology
Jet Propulsion Laboratory
Pasadena 4, California 1

Commanding Officer
Office of Naval Research
Navy 100, Fleet Post Office
New York, New York 1

Editor, Biblography of Technical Reports
Office of Technical Services
U. S. Dept. of Commerce
Washington 25, D. C. 1

Editor, Technical Data Digest
Armed Services Technical Information Agency
Document Service Center
U. B. Building
Dayton 2, Ohio 1

Editor, Engineering Index
29 West 39th Street
New York 18, N. Y.

Editor, Aeronautical Engineering Review
2 E. 64th Street
New York 21, N. Y. 1

Editor, Applied Mechanics Reviews
Midwest Research Institute
4049 Pennsylvania Avenue
Kansas City 2, Missouri 2

Technical Library
Lockheed Aircraft Corp.
2555 North Hollywood Way
Burbank, California 1

Technical Library
Pratt and Whitney Aircraft Div.
United Aircraft Corp.
East Hartford 8, Conn. 1

Technical Library
Glenn L. Martin Company
Baltimore 3, Maryland 1

Technical Library
Grumann Aircraft Engineering Corp.
Bethpage, Long Island, N. Y. 1

Technical Library
McDonnell Aircraft Corp.
Box 516
St. Louis 3, Missouri 1

Technical Library
North American Aviation, Inc.
12241 Lakewood Blvd.
Downey, California 1

Technical Library
Northrop Aircraft Company
1017 E. Broadway
Hawthorne, California 1

Prof. H. Emmons
Harvard University
Cambridge 38, Mass. 1